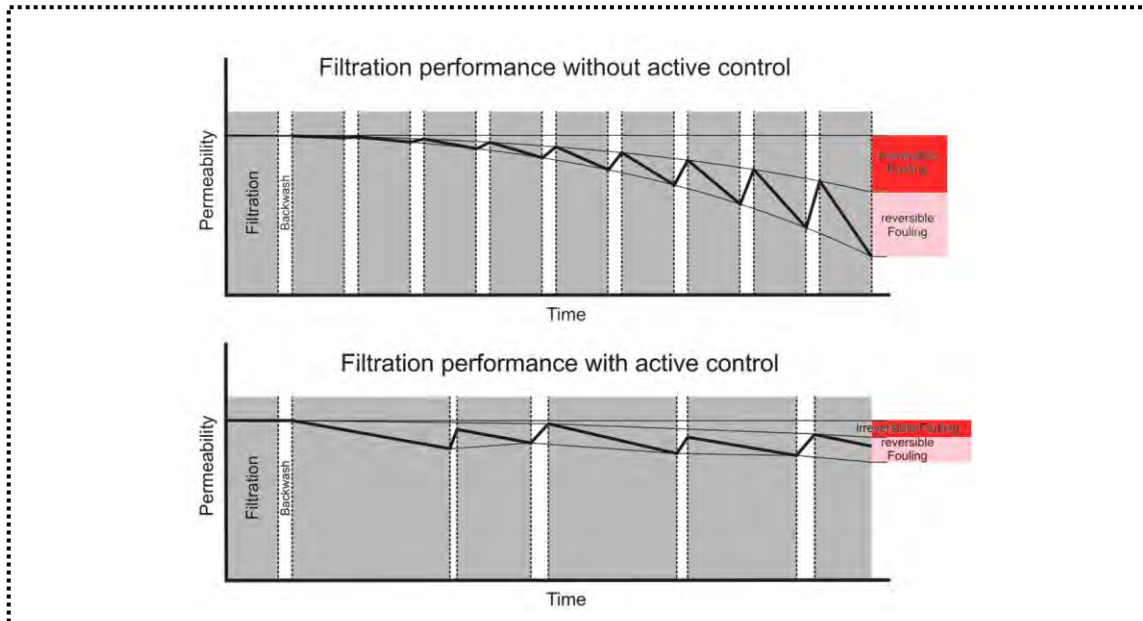


Use and benefit of ANCS at an ultrafiltration system



The research leading to these results has received funding from the European Union Seventh Framework Programme (FP7/2007-2013) under Grant Agreement no. 308339 for the research project DEMEAU

Title: Use and benefit of ANCS at an ultrafiltration system

Summary: An automatic neural net control system (ANCS) based on Artificial Neural Networks (ANN) was implemented at UF membrane filtration pilot plant in Roetgen to improve operational parameters filtration time and flux as well as backwash time and flux regarding the target parameters permeability at filtration start and filtration end. During this work period ANNs were improved and are discussed in detail considering the input parameter influences like operational parameters, temperature and turbidity on the target parameters.

Emanating from this offline optimization approaches, namely costs minimzation, productivity maximization and minimization of costs versus revenue, were developped and compared. Results show the benefit of productivity optimization as manipulable energy costs for reduction of TMP are insignificant compared to backwash costs. Possible savings amount to about 30 %.

Data from large scale plant UF membrane pilot plant for backwash water treatment were preprocessed to calculate characteristic filtration cycle parameters. With those data ANNs on basis of pilot plant data were validated. Generally, validation seems to be possible but due to differences in data ranges of large scale and pilot plant data validation showed significant deviations so that the models of the pilot plant could not be transferred to the large scale plant.

Grant agreement no:	308339
Work Package:	WP23
Deliverable number:	D23.3
Partner responsible:	aquatune
Deliverable author(s):	Silke Mueller, Joerg Gebhardt
Quality assurance:	Thomas Wintgens (FHNW), Erwin Beerendonk (KWR)
Planned delivery date:	28.02.2014
Actual delivery date:	31.03.2015
Dissemination level:	PU

© 2012 DEMEAU

This Demonstration project 'Demonstration of promising technologies to address emerging pollutants in water and waste water' (DEMEAU) has received funding from the European Union's Seventh Programme for Research, Technological Development and Demonstration under Grant Agreement no. 308330. All rights reserved. No part of this book may be reproduced, stored in a database or retrieval system, or published, in any form or in any way, electronically, mechanically, by print, photograph, microfilm or any other means without prior written permission from the publisher.

This publication reflects only the author's views and the European Union is not liable for any use that may be made of the information contained therein.

Table of contents

LIST OF ACRONYMS	III
LIST OF FIGURES	IV
LIST OF TABLES.....	VI
SUMMARY	1
1 TASK DESCRIPTION	3
1.1 <i>Abstract of the Plant/ Process</i>	3
1.1.1 Pilot Plant	3
1.1.2 Large Scale Plant	5
1.2 <i>Task description and targets of the project</i>	5
2 MODELLING BACKWASH AND FILTRATION	7
2.1 <i>Analysis of data</i>	7
2.2 <i>Training of the models</i>	10
2.3 <i>Validation of the models</i>	12
2.3.1 Model of Filtration Subcycle (Target Parameter UF_NPERMe)	12
2.3.2 Model of Backwash Subcycle (Target Parameter UF_NPERMs).....	14
2.4 <i>Analysis of the Models</i>	16
2.4.1 Manipulable Variable Filtration Time.....	16
2.4.2 Manipulable Variable Backwash Time	17
2.4.3 Manipulable Variable Flow Rate	18
2.4.4 Manipulable Variable Backwash Flow rate	18
2.4.5 Disturbance Variable NPERMe_m1 and NPERMs	19
2.4.6 Disturbance Variable Temperature.....	20
2.4.7 Disturbance Variable Turbidity Load Since Last CEB.....	22
2.5 <i>Transfer of the results on the large scale plant</i>	23
2.5.1 Model of Filtration Subcycle (Target Parameter UF_NPERMe)	24
2.5.2 Model of Backwash Subcycle (Target Parameter UF_NPERMs).....	27
2.5.3 Conclusion for the transferability to the large scale plant	28
3 DESIGN OF THE OPTIMIZATION SYSTEM	31

3.1	<i>The Genetic Optimizer</i>	31
3.2	<i>Optimization Strategy</i>	32
3.3	<i>Optimization results</i>	34
4	CONCLUSIONS	42
	REFERENCES.....	43

List of Acronyms

ANCS	Automatic Neural Net Control System
ANN	Artificial Neural Network
APC	Advanced Process Control
CEB	Chemical Enhanced Backwash
GA	Genetic algorithm
UF	Ultrafiltration
WAG	Wassergewinnungs- und aufbereitungsgesellschaft Nordeifel mbH

List of Figures

Figure 1:	Development of the membrane permeability over a number of filtration and backwash periods.....	1
Figure 2:	Schematic of the Plant UF100 (Screenshot of the SCADA system)	3
Figure 3:	Program structure of UF filtration pilot plant	4
Figure 4:	Scheme of the backwash water treatment plant.....	5
Figure 5:	The Optimization Strategy.....	6
Figure 6:	Permeability and Transmembrane Pressure of UF100 as a Function of Time	7
Figure 7:	Permeability and Transmembrane Pressure of UF200 as a Function of Time	8
Figure 8:	Filtration Flow and Time of UF100 and UF200 as a Function of Time.....	8
Figure 9:	Backwash Flow and Time of UF100 and UF200 as a Function of Time	9
Figure 10:	Filtration cycle with indication of start and end permeabilities	10
Figure 11:	Structure of the Filtration and Normal Backwash Model (Left: Target Parameter End Permeability, Right: Target Parameter Start Permeability).....	11
Figure 12:	Validation of Filtration Model (Target Parameter: End Permeability) with the training data set (Datensätze).....	12
Figure 13:	Correlation Graph of Start Permeability (ANN prediction (Vorhersage) plotted against measured value (Ausgangswert))	13
Figure 14:	Frequency Distribution of Error Classes of End Permeability showing the number of deviations (Anzahl) against the deviation in % of data range (Abweichung [% vom Wertebereich])	13
Figure 15:	Validation of Backwash Model (Target Parameter: Start Permeability) with the training data set (Datensätze).....	14
Figure 16:	Correlation Graph of Start Permeability (ANN prediction (Vorhersage) plotted against measured value (Ausgangswert))	15
Figure 17:	Frequency Distribution of Error Classes of End Permeability showing the number of deviations (Anzahl) against the deviation in % of data range (Abweichung [% vom Wertebereich])	15
Figure 18:	Sensitivity Curves of Filtration Time, Target Parameter End Permeability	16
Figure 19:	Sensitivity Curves of the Backwash Time, Target Parameter Start Permeability	17
Figure 20:	Sensitivity Curve of the Filtration Flow Rate, Target Parameter End Permeability	18

Figure 21:	Sensitivity Curve of the Backwash Flow Rate, Target Parameter Start Permeability.....	19
Figure 22:	Sensitivity Curves of start Permeability of the filtration run, Target Parameter End Permeability.....	19
Figure 23:	Sensitivity Curves of end permeability of preceding filtration cycle, Target Parameter Start Permeability	20
Figure 24:	Sensitivity Curves of Temperature, Target Parameter End Permeability.....	21
Figure 25:	Sensitivity Curves of Temperature, Target Parameter Start Permeability	21
Figure 26:	Sensitivity Curves of Turbidity Load since Last CEB, Target Parameter End Permeability	22
Figure 27:	Sensitivity Curves of Turbidity Load since Last CEB, Target Parameter Start Permeability	23
Figure 28:	Validation of Filtration Model (Target Parameter: End Permeability) for large scale data.....	25
Figure 29:	Correlation Graph of Start Permeability for large scale data	25
Figure 30:	Frequency Distribution of Error Classes of End Permeability for large scale data	26
Figure 31:	Validation of Backwash Model (Target Parameter: Start Permeability) for large scale data.....	27
Figure 32:	Correlation Graph of Start Permeability for large scale data	28
Figure 33:	Frequency Distribution of Error Classes of End Permeability for large scale data	28
Figure 34:	Validation of Filtration Model (Target Parameter: End Permeability) after retraining with large scale data	29
Figure 35:	Correlation Graph of Start Permeability for large scale data after retraining with large scale data	29
Figure 36:	Frequency Distribution of Error Classes of End Permeability for large scale data after retraining with large scale data	30
Figure 37:	Genetic Optimizer.....	32
Figure 38:	Scheme illustrating costs and gain during a filtration cycle.....	33
Figure 39:	Optimization of filtration time.....	36
Figure 40:	Optimization of filtration flow	37
Figure 41:	Optimization of backwash time.....	37
Figure 42:	Optimization of backwash flow	38
Figure 43:	Measured and resulting permeability at filtration end	39
Figure 44:	Measured and resulting permeability at filtration start.....	39
Figure 45:	Productivity before and after optimization.....	40

List of Tables

Table 1:	Results of the Modelling.....	11
Table 2:	Data Ranges of Pilot and Large Scale Plant	24
Table 3:	Results of Modelling with Large Scale Data.....	28
Table 4:	Optimization results (Filtrated Water amounts to about 4.3 Mio. m ³ /a)	35
Table 5:	Summary of the optimization results with respect to the real settings.....	40

Summary

Membrane filtration is a complex process of altering filtration and backwash cycles with process performance being strongly depending on raw water quality. To ensure high performance process operation parameters as filtration and backwash flux as well as filtration and backwash duration have to be frequently adjusted taking changing raw water conditions into account. For automated process control an automatic neural net control system (ANCS) based on artificial neural networks (ANN) and genetic algorithms (GA) was developed in EU-Life project “Purifast” (Purifast 2012). Assuming that actual raw water conditions also influence subsequent filtration/backwash cycles new optimal operation parameters are generated taking the actual process performance in terms of membrane permeability into account.

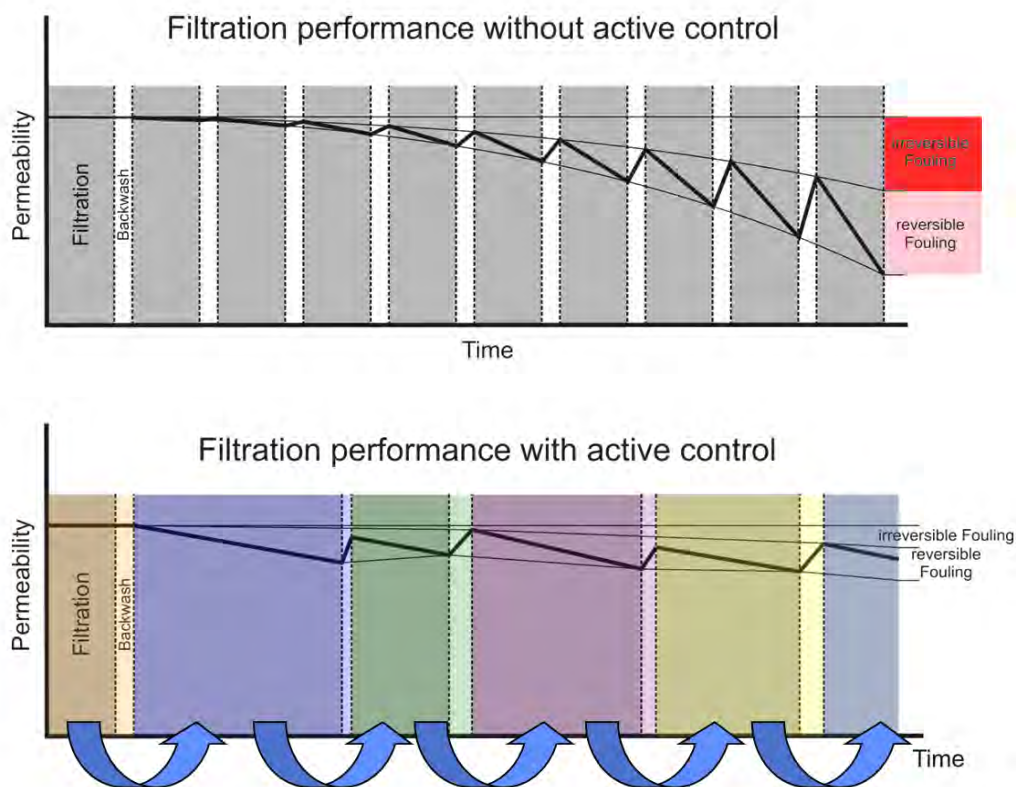


Figure 1: Development of the membrane permeability over a number of filtration and backwash periods

Based on characteristic filtration cycle parameters like permeability at filtration start and end, filtration and backwash flow, filtration and backwash time, average temperature and turbidity load ANNs are trained and implemented in ANCS. The control system gives optimization proposals for the manipulable variables filtration and backwash flow as well as filtration and backwash time thus individually adjusting filtration

and backwash parameters due to changing raw water conditions and process performance of the preceding filtration cycle to reduce irreversible fouling to a minimum and optimize operational costs (cf. Figure 1).

Within this reporting period ANNs were retrained to improve accuracy and again validated and analysed intensively. Models ought to be transferred to the large scale backwash water treatment plant but data ranges of both plants differed significantly so that validation of the pilot plant model with large scale data hypothesizes transferability but it could not finally be proven. Therefore ANCS was tested offline for pilot plant data from March 2014 to March 2015 with three different optimization approaches (costs minimization, productivity maximization and minimisation of costs versus revenue) showing a potential cost reduction of about 30 %.

1 Task Description

1.1 Abstract of the Plant/ Process

1.1.1 Pilot Plant

The equipment of the DEMEAU-project consists of two dead end UF membrane filtration plants (inside-out multi-bore system with 1 m² membrane surface each), referred to as UF100 and UF200. The raw water flows to the ultrafiltration plants with a certain pressure. It enters the installation either from the top or from the bottom (see Figure 2). The transmembrane pressure TMP is converted to the permeability by dividing it by the measured flux. Permeability is the parameter that describes the state of the membranes in a way that is well suited for optimisation.

Both plants are operated by switching between 6 process-states. As shown in Figure 2 water can enter the membrane module at the top or at the bottom. By altering flow direction across the membrane uniform loading can be achieved. The resulting modes are called “filtration top”, “filtration bottom”, “backwash top”, “backwash bottom” and CEB (Chemically Enhanced Backwash) part one (alkalinous) and part two (acid).

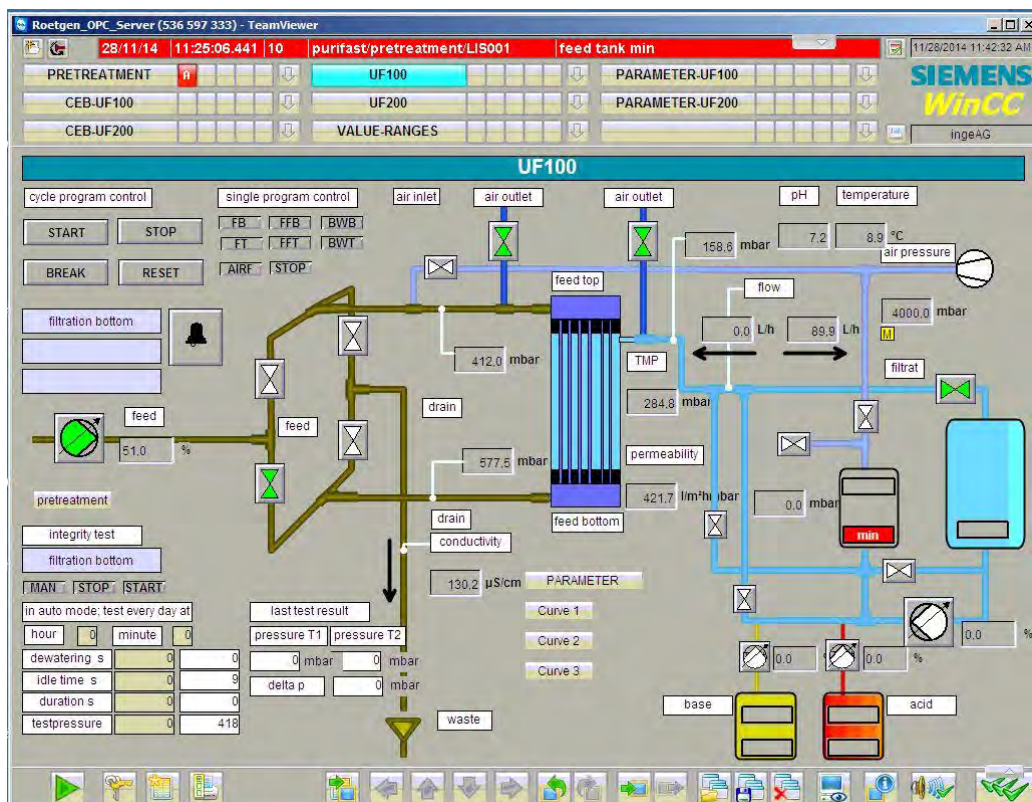


Figure 2: Schematic of the Plant UF100 (Screenshot of the SCADA system)

Each filtration is followed by a backwash to recover from the reversible part of the loss in permeability. As depicted in Figure 1 only part of permeability loss can be restored by backwashing while another part remains as permanent loss (irreversible fouling). Therefore from time to time a CEB is applied (duration is approx. 1 to 2 hours) to recover from the irreversible part of the permeability loss. The CEB starts with the application of sodium hydroxide, followed by sulphuric acid.

Figure 3 shows the program structure of a single filtration unit. To distinguish the different steps in data collection a status signal is delivered.

Process steps	times		
Filtration 1		Filtration bottom	
Filtration bottom min	45		
Filtration top min	0		
Forward Flush 1.1			
Fwd Flush bottom s	0	Backwash bottom	
Fwd Flush top s	0		
Backwash 1		Fwd Flush bottom	
Backwash bottom s	60		
Backwash top s	0	Filtration top	
Forward Flush 1.2			
Fwd Flush bottom s	30		
Fwd Flush top s	0		
Filtration 2		Backwash top	
Filtration bottom min	0		
Filtration top min	45	Fwd Flush top	
Forward Flush 2.1			
Fwd Flush bottom s	0	After each programm cycle -> CEB-Counter Z=Z+1 (CEB at Z=x)	
Fwd Flush top s	0		
Backwash 2			
Backwash bottom s	0		
Backwash top s	60		
Forward Flush 2.2			
Fwd Flush bottom s	0		
Fwd Flush top s	30		

Figure 3: Program structure of UF filtration pilot plant

1.1.2 Large Scale Plant

Drinking water treatment at WAG Wassergewinnungs- und aufbereitungsgesellschaft Nordeifel mbH (below WAG) in Roetgen is a two stage UF membrane process consisting of the drinking water treatment plant followed by a backwash water treatment step. As the productivity of the drinking water treatment plant is lower than expected, a higher amount of backwash water has to be treated in the backwash water treatment step. To increase the capacity of the plant, extension either by new modules or increase of membrane surface area is planned. Optimization with ANCS can help to increase the capacity of the backwash water treatment plant and therefore reduce investment costs for a plant extension.

Figure 4 shows a scheme of the backwash water treatment plant. Influent is the backwash water of the drinking water treatment plant. The process itself is directly comparable to the pilot plant. The backwash water is treated by thickening and dewatering prior to disposal of the sludge to a landfill. The clear water of the clarifier is discharged to the receiving water. The filtrate of the backwash water treatment plant is lead back to drinking water treatment plant.

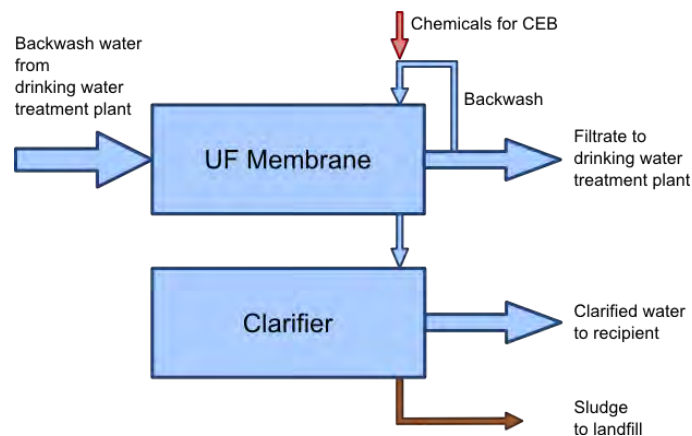


Figure 4: Scheme of the backwash water treatment plant

1.2 Task description and targets of the project

The main target of this project is to keep the permeability high in order to achieve minimum energy consumption (high permeability corresponds to low pressure which again corresponds to low energy consumption). This is done by applying backwash cycles (normal and CEB). The trade-off is that backwashes consume water and thus reduce productivity. The optimizer has to find the best compromise between energy consumption and productivity. Particularly the CEB are very expensive due to the application of chemicals and the big loss in productivity caused by the duration of about 1 to 2 hours. The principle of an optimization system as applied in ANCS is shown in Figure 5.

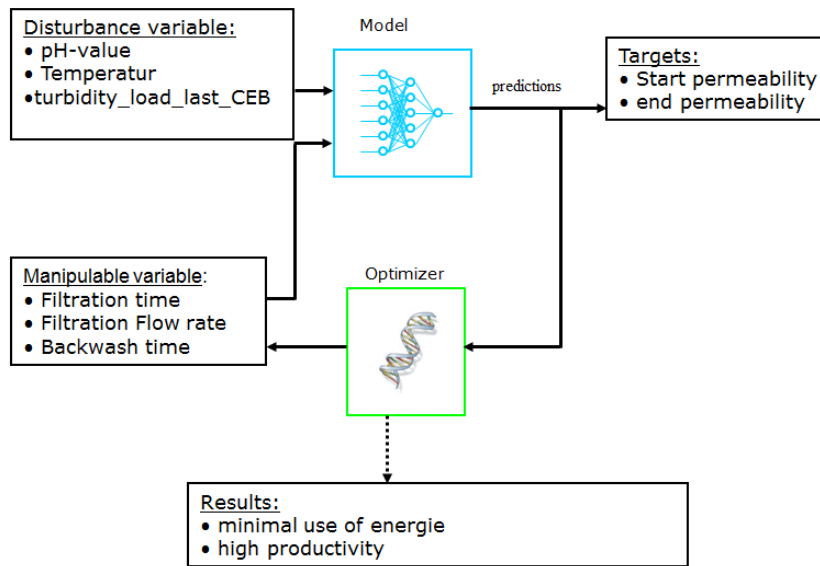


Figure 5: The Optimization Strategy

2 Modelling Backwash and Filtration

2.1 Analysis of data

Before the data can be used for the training of models they have to be processed. This is done by the data pre-processing block in APC professional, the engineering environment which organizes the complete dataflow between the genetic optimizer, the ANN and the human machine interface. The incoming signals are averaged and then sampled at different points in time, depending on which subcycle (filtration, backwash, CEB) is under consideration. The permeability is calculated from the pressure measurements, averaged and sampled at the end of a filtration subcycle (“end permeability”) and at the end of a backwash subcycle (“start permeability”). The terms “start” and “end” refer to the start and ending points of a filtration cycle.

The diagrams in Figure 6 to Figure 9 show the behaviour of the start- and end- permeability along with the corresponding transmembrane pressure TMP, filtration and backwash flow UF_Q and UF_BW_Q respectively as well as filtration and backwash times UF_Filt_t and UF_BW_t, originating from March 2014 to March 2015. Backwash times are only shown for normal backwash, not for CEB.

In ZR3 unfortunately a large data gap occurred due to unstable data transfer from the WinCC system to the ANCS PC for several variables. Though historical data were also collected on the WinCC system it was decided to keep the preprocessed data from APC as it allows a more precise data compression to characteristic parameters according to the higher sampling rate compared to the stored WinCC data.

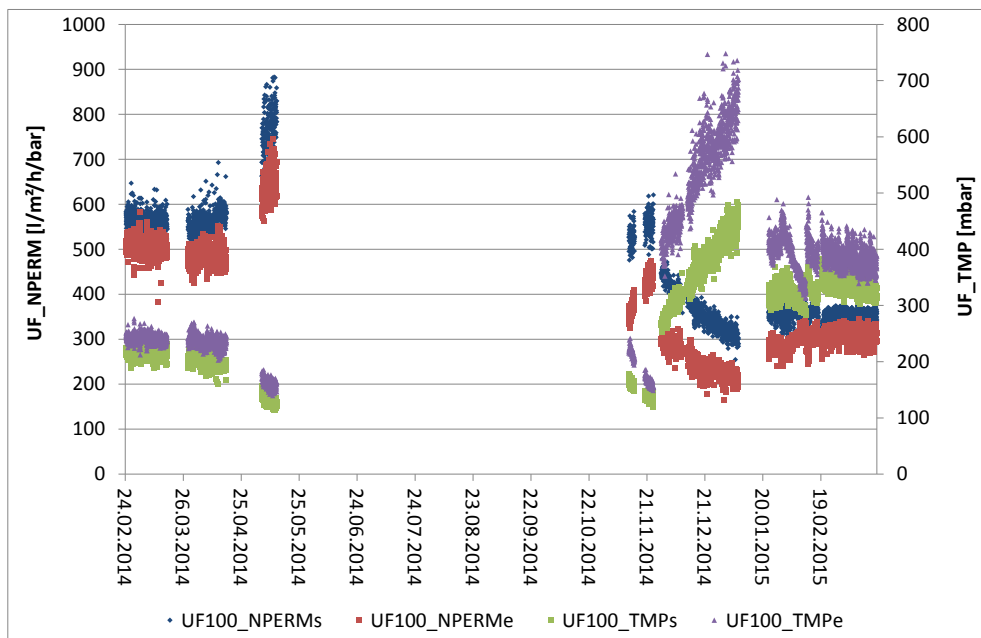


Figure 6: Permeability and Transmembrane Pressure of UF100 as a Function of Time

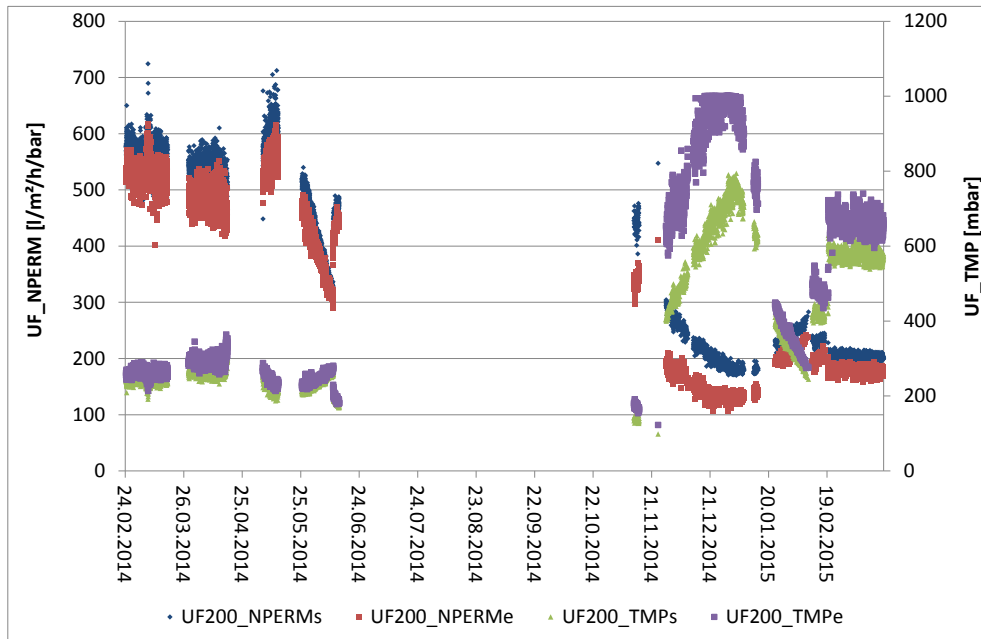


Figure 7: Permeability and Transmembrane Pressure of UF200 as a Function of Time

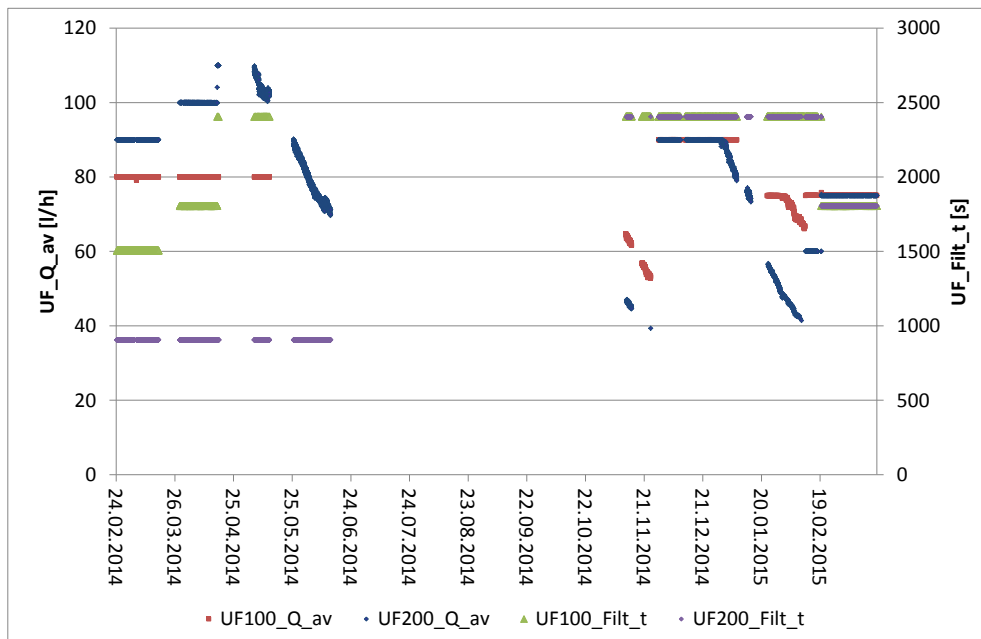


Figure 8: Filtration Flow and Time of UF100 and UF200 as a Function of Time

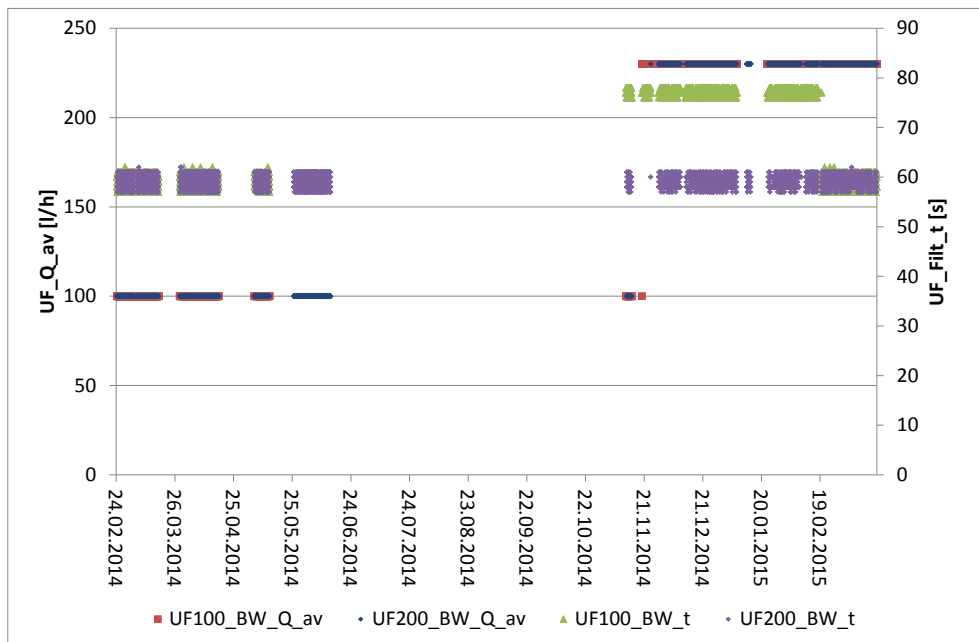


Figure 9: Backwash Flow and Time of UF100 and UF200 as a Function of Time

The blue and red curves in Figure 6 and Figure 7 show the start- and the end permeability, the green and purple curves show the start- and end transmembrane pressure, while the red and blue curves in Figure 8 and Figure 9 represent the flow rates for filtration and backwash respectively. The green and purple curves show the duration of filtration and backwash without CEB. The flow rate is adjusted by the operators while the pressure results from this adjustment. The permeability is calculated from pressure and flow rate. It is a membrane property, which changes due to the change in operating conditions.

The period of May to June shows a decline in permeability. Although the flow rate is reduced continuously, the pressure increases because of a decreasing permeability. This means that the backwash procedure (including CEB, which is not shown in Figure 9) was not able to maintain a high permeability condition. This situation has to be avoided in order to operate the process under optimum conditions.

The time period from end of October to end of November shows comparatively good values for the permeability, which allowed operation at reduced energy consumption. But the price for this was a reduced productivity, because the high permeabilities were achieved by reducing the filtration flow rate and mainly by increasing backwash flow rate and duration.

2.2 Training of the models

This chapter discusses the created models of the filtration process for regular backwash. CEB was modelled and analysed separately. Figure 10 indicates the permeabilities with respect to data logging.

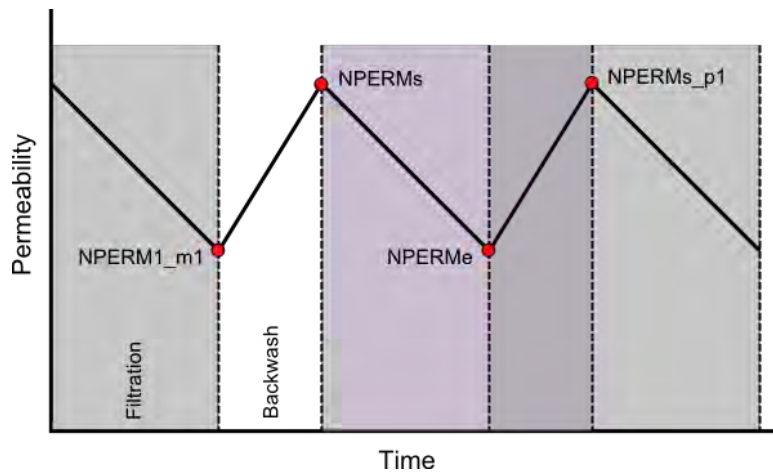


Figure 10: Filtration cycle with indication of start and end permeabilities

The chosen target parameters for the neural networks (ANN) are permeability at filtration end (NPERMe) and start permeability (NPERMs_p1) after backwash. Both parameters are affected by the temperature, pH-value and turbidity_load_last_CEB (accumulated turbidity load since the last application of a CEB) whereupon pH-value was kept constant during sampling period and can therefore be neglected. Filtration time and filtration flow rate are used as inputs to the filtration models (end permeability), while backwash time and backwash flow rate are used as inputs to the backwash models (start permeability).

Figure 11 shows the structure of the trained ANNs for the filtration subcycle with its input- and output signals. The meaning of the signals is discussed in chapter 3.2 “Analysis of the Models”.

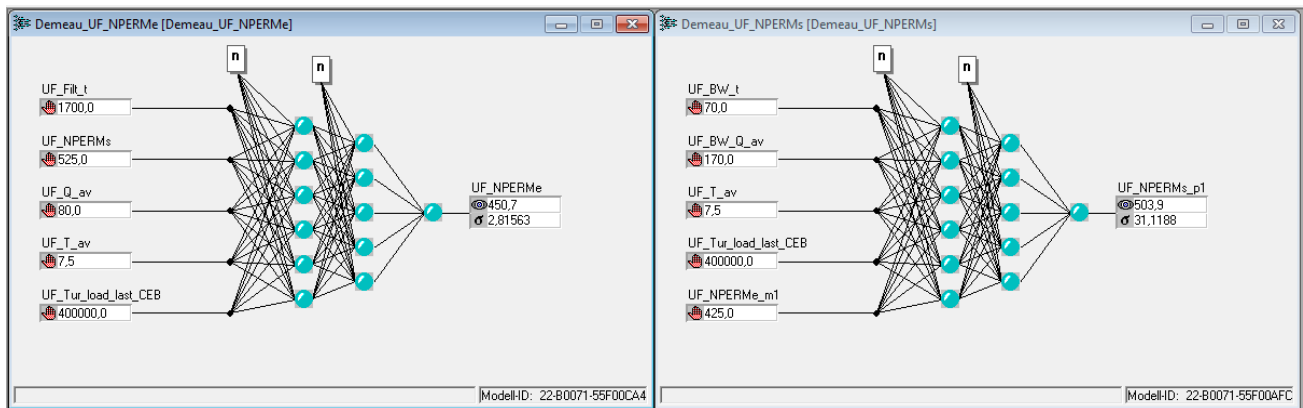


Figure 11: Structure of the Filtration and Normal Backwash Model (Left: Target Parameter End Permeability, Right: Target Parameter Start Permeability)

Since the two equal membrane modules UF100 and UF200 were operated with different settings of parameters, the data were combined to one database, which was used to develop a so called “combi model”. The necessary condition that both membrane modules behave in a similar way was tested by validating the models for UF100 with UF200 data and reverse. By those validations the condition was found to be fulfilled. With this approach the amount of patterns learned by the ANNs could be increased and a more generic model was developed. The finally used models are shown in Table 1:

Table 1: Results of the Modelling

Name	ID	Date	Mean deviation	Mean absolute deviation	Sigma	RSQ
Demeau_UF_NPERMe	22-B0071-55F00CA4	09.09.2015	0.06%	1.28%	1.99%	0.99
Demeau_UF_NPERMs	22-B0071-55F00AFC	09.09.2015	-0.38%	1.82%	3.08%	0.99

All deviations are given in relation to the data range of the particular output. Sigma represents the standard deviation of forecast error and the RSQ is the linear correlation coefficient. As a rule of thumb resulting from practical experiences of hundreds of modelling runs it can be said, that values of sigma < 10 % and RSQ > 0,8 indicate useful models.

2.3 Validation of the models

The validation is the process of testing the accuracy and validity of models. The following diagrams from Figure 12 to Figure 17 show the validation for all used models. The green curves show the measured values and the blue curves represent the calculated model predictions. The percentages refer to the respective ranges of values of the target parameters. The target parameters are plotted over datasets. Though it looks like time-series graphs there is no real time dependency as the validation is shown for training data which are clustered prior to modelling. Nevertheless this delivers an easy accessible representation of validation results.

Additionally correlation graph and frequency distribution of error classes are shown.

2.3.1 Model of Filtration Subcycle (Target Parameter UF_NPERMe)

Overall the ANN for prediction of end permeability NPERMe shows a sufficiently accurate validation with some higher deviations in the middle data range.

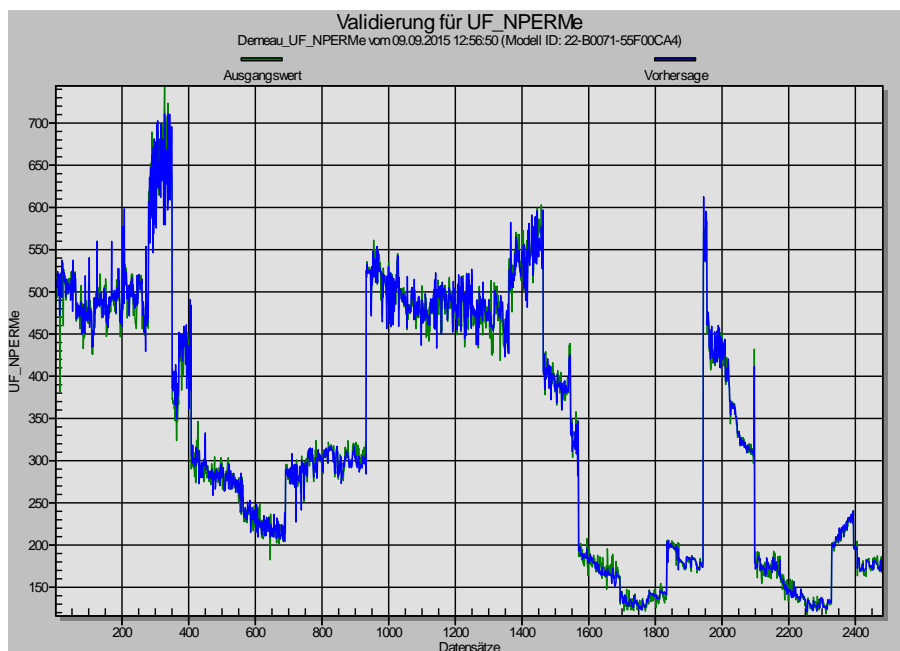


Figure 12: Validation of Filtration Model (Target Parameter: End Permeability) with the training data set (Datensätze)

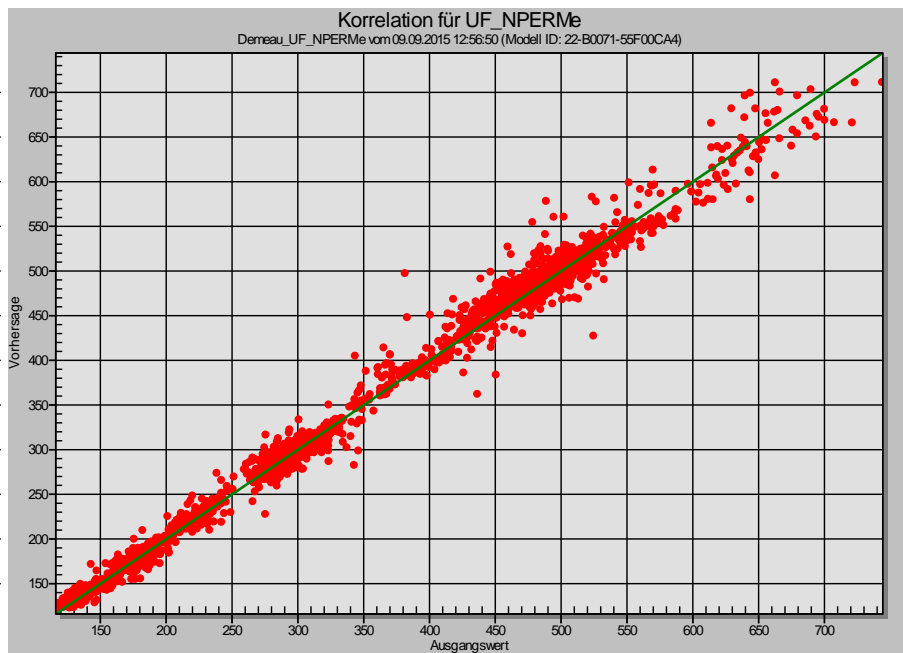


Figure 13: Correlation Graph of Start Permeability (ANN prediction (Vorhersage) plotted against measured value (Ausgangswert))

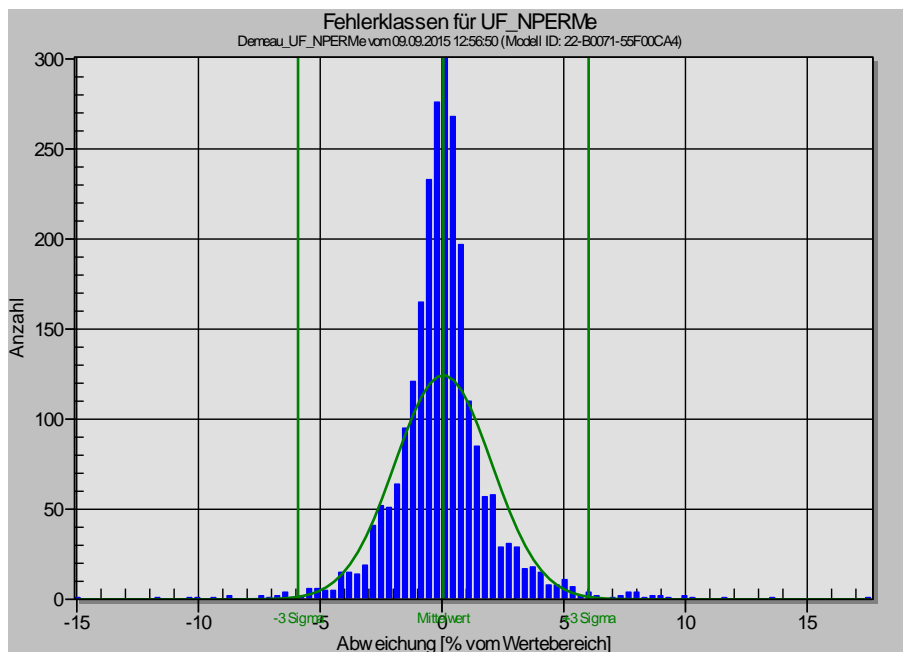


Figure 14: Frequency Distribution of Error Classes of End Permeability showing the number of deviations (Anzahl) against the deviation in % of data range (Abweichung [% vom Wertebereich])

2.3.2 Model of Backwash Subcycle (Target Parameter UF_NPERMs)

As for end permeability the ANN for start permeability delivers sufficient prediction quality with some higher deviations in the upper data range.

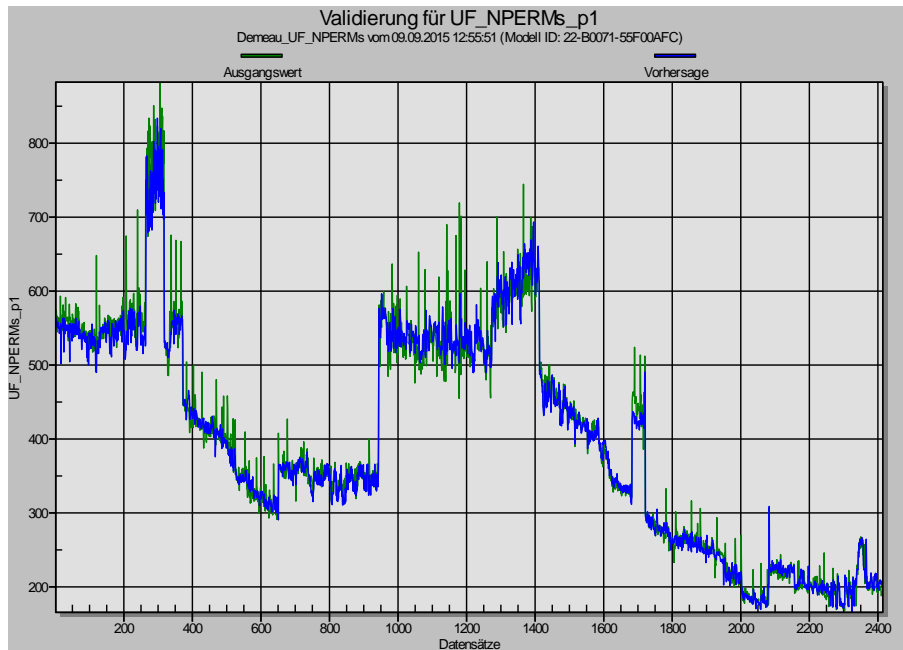


Figure 15: Validation of Backwash Model (Target Parameter: Start Permeability) with the training data set (Datensätze)

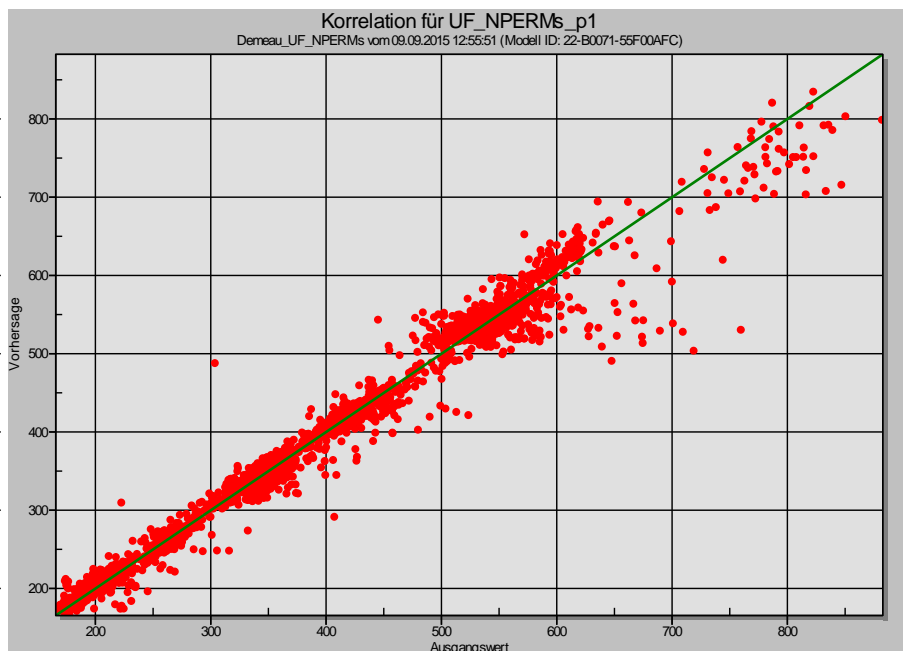


Figure 16: Correlation Graph of Start Permeability (ANN prediction (Vorhersage) plotted against measured value (Ausgangswert))

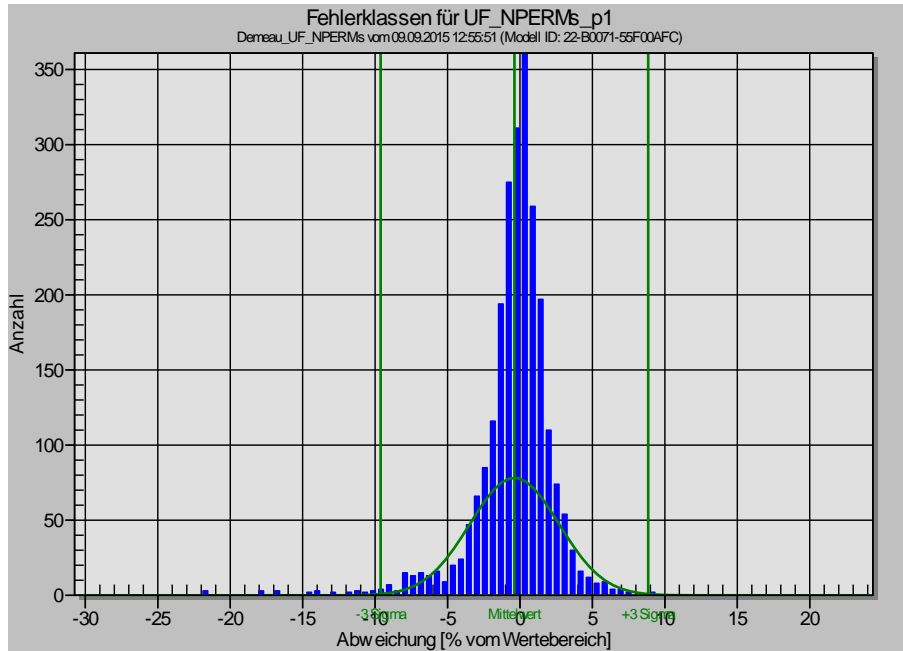


Figure 17: Frequency Distribution of Error Classes of End Permeability showing the number of deviations (Anzahl) against the deviation in % of data range (Abweichung [% vom Wertebereich])

2.4 Analysis of the Models

This chapter discusses the relations between the input signals (disturbance variables and manipulable variables) and the output signals (target values), as the offline analysis of the models reveal them to us. Each of the following diagrams shows the answer of the ANN for 100 randomly selected data points when one input variable is varied over its data range. The result is 100 curves that show the effect of the selected parameter on the target parameter. On each curve the data point as starting point for variation is marked with an “x”. The curves are mostly green but can change their colour to red which illustrates a wide confidence interval of prediction. The best prediction quality is reached around the sampling points so that the interpretation of the gradient at those points delivers the most confidential relation between input and target parameter.

2.4.1 Manipulable Variable Filtration Time

One of the most important influential variables is the filtration time. The little crosses in the diagram show, that there were two different settings for this variable in the database used for the training: one setting equals 900 seconds and the other setting equals 2400 seconds. The form of the curves between those values is interpolated by the model.

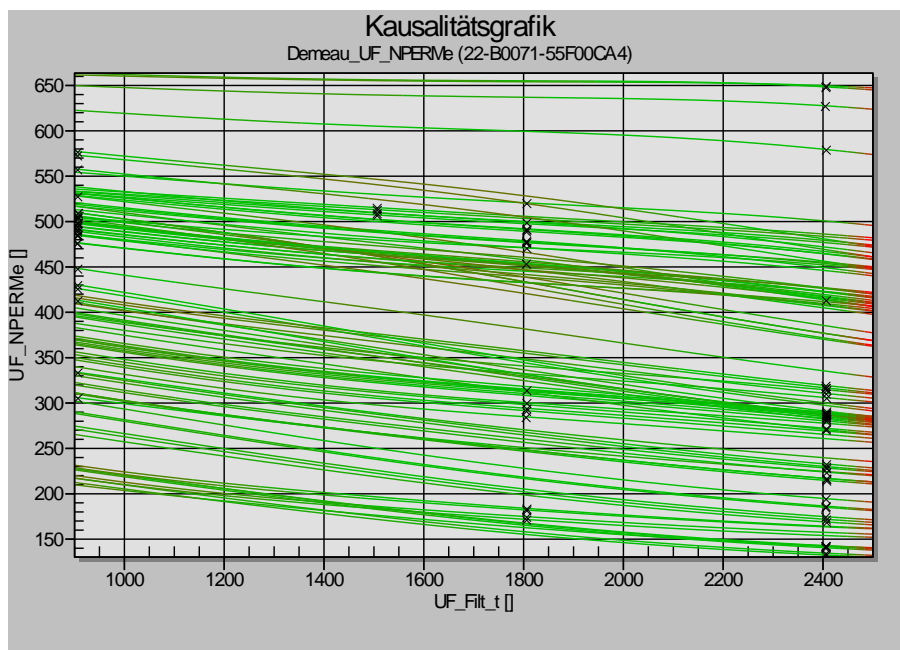


Figure 18: Sensitivity Curves of Filtration Time, Target Parameter End Permeability

The diagram shows the connection of longer filtration times with reduced end permeability. This result seems to be plausible, since in the course of filtration the membrane is more and more loaded with particles, which effectively reduces the permeability.

2.4.2 Manipulable Variable Backwash Time

During the backwash subcycle, the duration of the backwash (backwash time) is expected to improve the resulting start permeability. A behaviour, that is clearly shown by the curves of Figure 19.

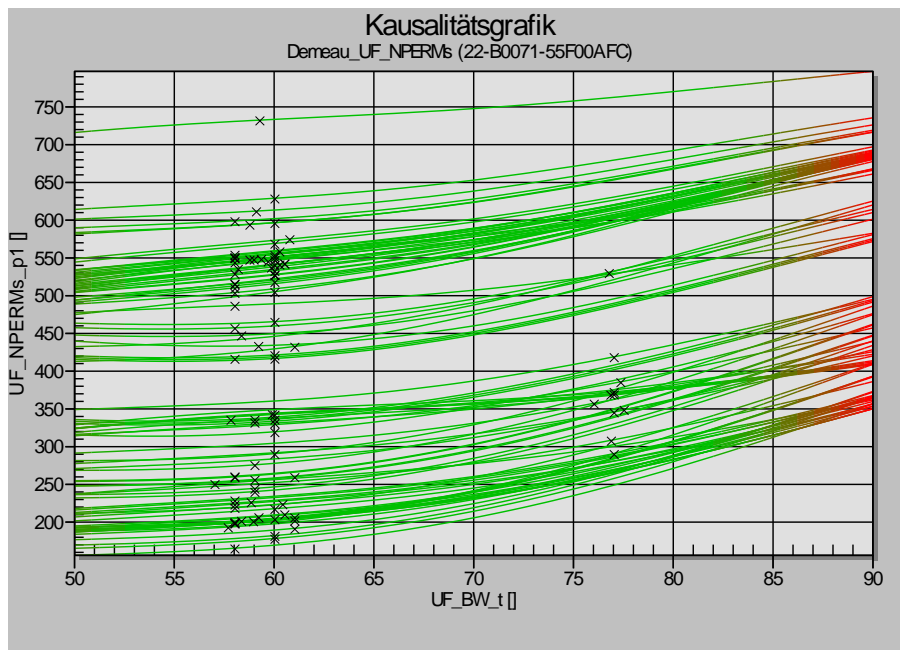


Figure 19: Sensitivity Curves of the Backwash Time, Target Parameter Start Permeability

The backwash time of both plants was normally set to values between 55 seconds and 60 seconds. In the case of two consecutively executed backwashes (Top and Bottom, cf. chapter 1.1.1 and Figure 2) we got longer times of 75 seconds.

The diagram confirms the expected behaviour, that the resulting permeability (start permeability) could be improved by longer backwash times, which would lead to reduced energy consumption of the system.

2.4.3 Manipulable Variable Flow Rate

Very interesting is of course the applied flow rate (which corresponds directly to the flux, because the area of the membrane equals 1 m²). This parameter can be adjusted and the following diagram shows, that higher values decrease the resulting permeability.

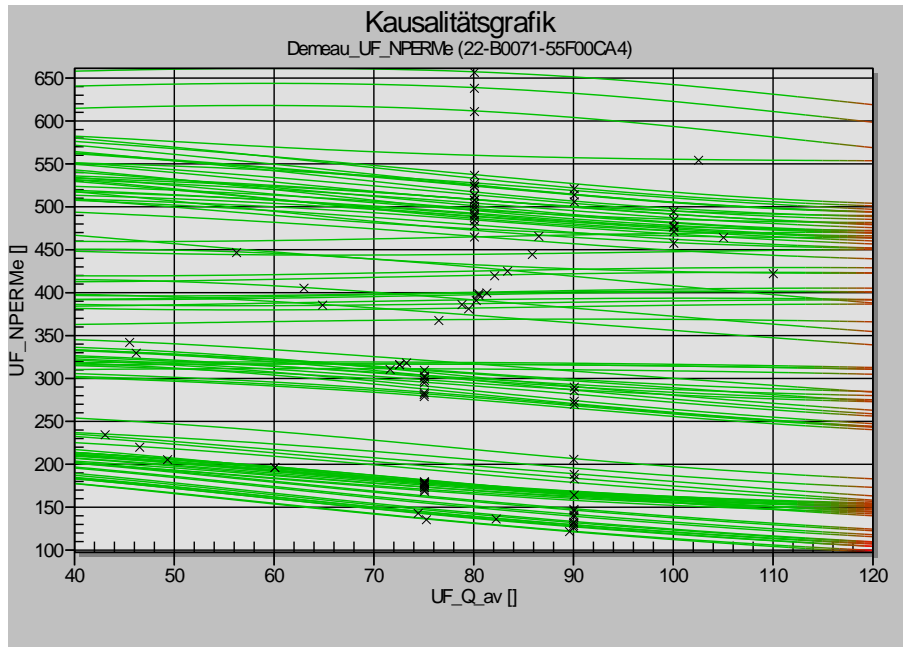


Figure 20: Sensitivity Curve of the Filtration Flow Rate, Target Parameter End Permeability

2.4.4 Manipulable Variable Backwash Flow rate

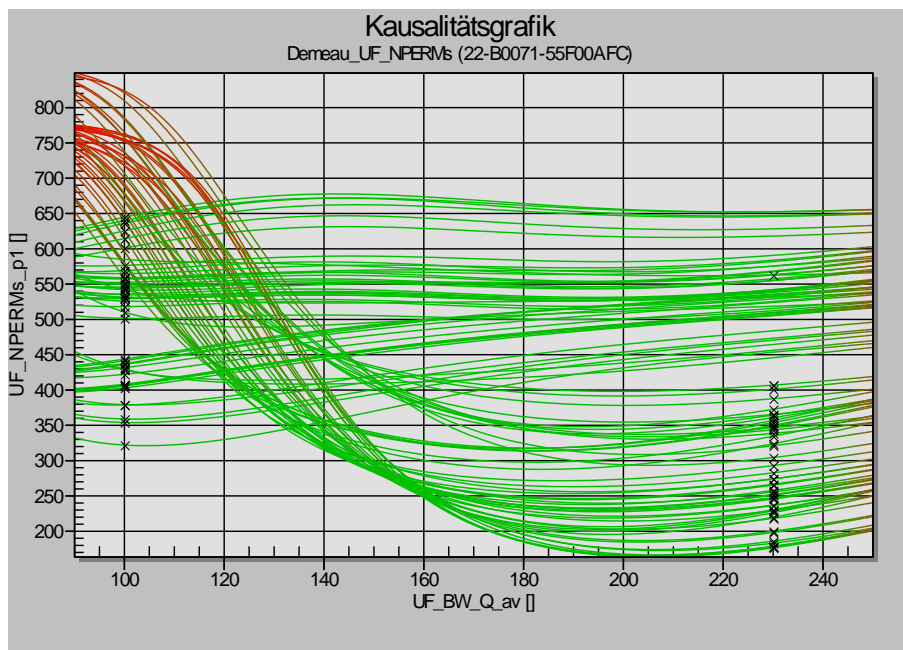


Figure 21: Sensitivity Curve of the Backwash Flow Rate, Target Parameter Start Permeability

Backwash flow rate appears to be less effective for increasing start permeability than backwash duration though a slight positive gradient can be found especially for high flow rate.

2.4.5 Disturbance Variable NPERMe_m1 and NPERMs

For prediction quality and clustering process prior to modelling inclusion of previous permeabilities is reasonable though those parameters will superimpose influences especially of temperature and turbidity load as the ANN-input permeabilities themselves are dependent on them. As expected permeability inputs show strong positive influence on the outputs.

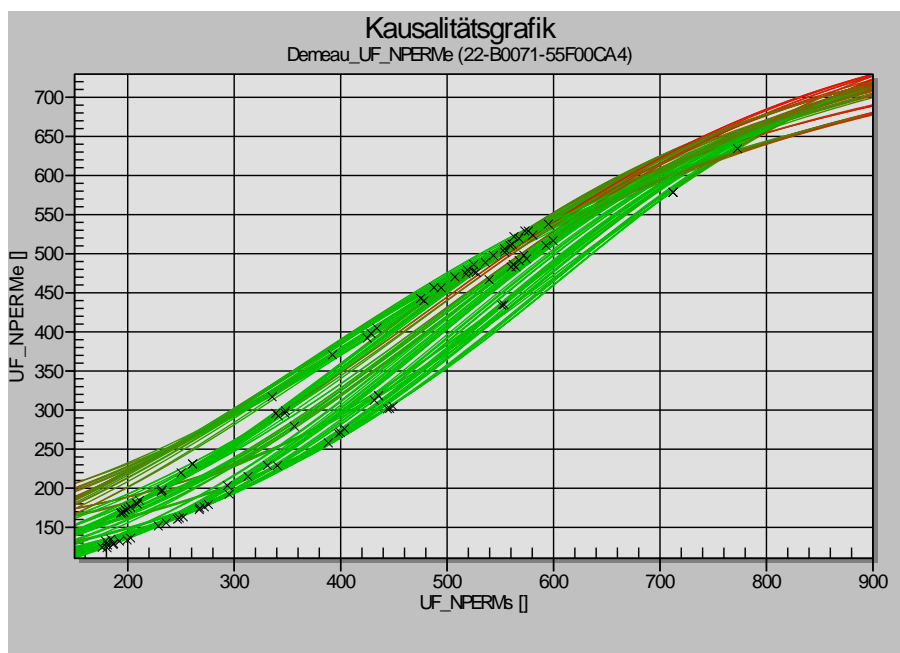


Figure 22: Sensitivity Curves of start Permeability of the filtration run, Target Parameter End Permeability

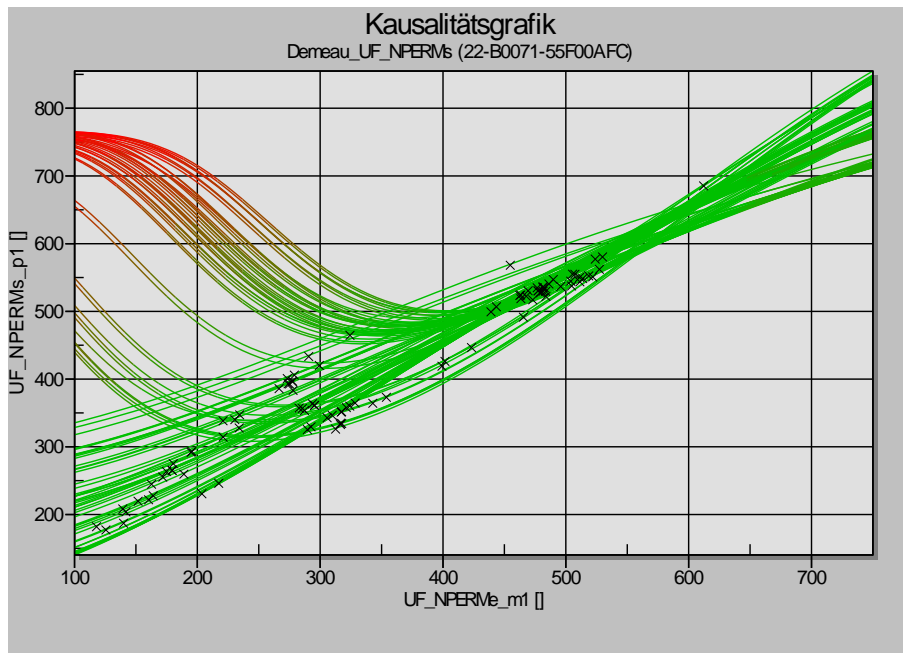


Figure 23: Sensitivity Curves of end permeability of preceding filtration cycle, Target Parameter Start Permeability

2.4.6 Disturbance Variable Temperature

The model shows no significant relation of temperature to the resulting permeability. This is also the case due to inclusion of permeability values as model inputs

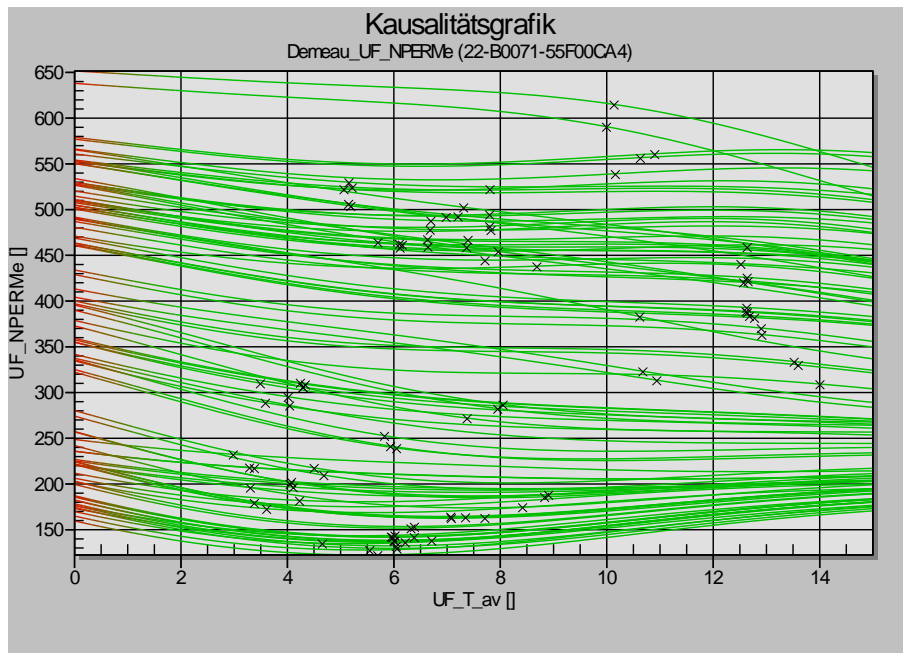


Figure 24: Sensitivity Curves of Temperature, Target Parameter End Permeability

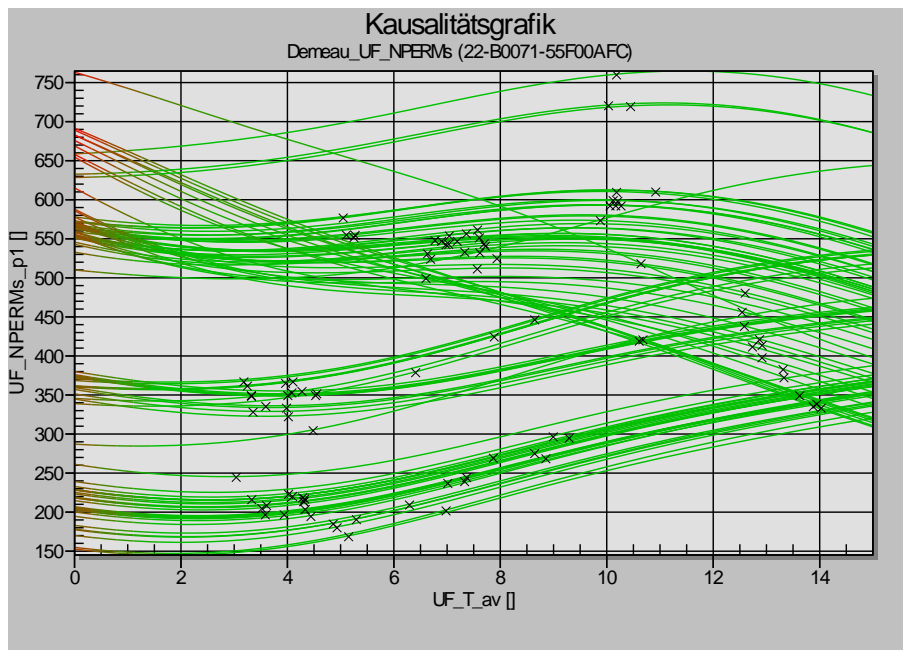


Figure 25: Sensitivity Curves of Temperature, Target Parameter Start Permeability

Mostly the start permeability of the backwash model increases with growing temperatures. This seems to be plausible, because the permeability values we used were not corrected for temperature influences on viscosity. In some cases for high temperatures also a negative influence appears.

2.4.7 Disturbance Variable Turbidity Load Since Last CEB

Turbidity_load_last_CEB is the summation of the turbidity loads of every filtration within a valid cycle since last CEB. This parameter supplies us with a good measure for the load to which the membrane is exposed.

The turbidity load is calculated in the block “data pre-processing” in APC by means of the following function:

$$\text{turbidity load} = \frac{\text{Turbidity} * \text{flow rate} * \text{Filtration time}}{3600}$$

This parameter is also very important for modelling, particularly for the start permeability after a backwash.

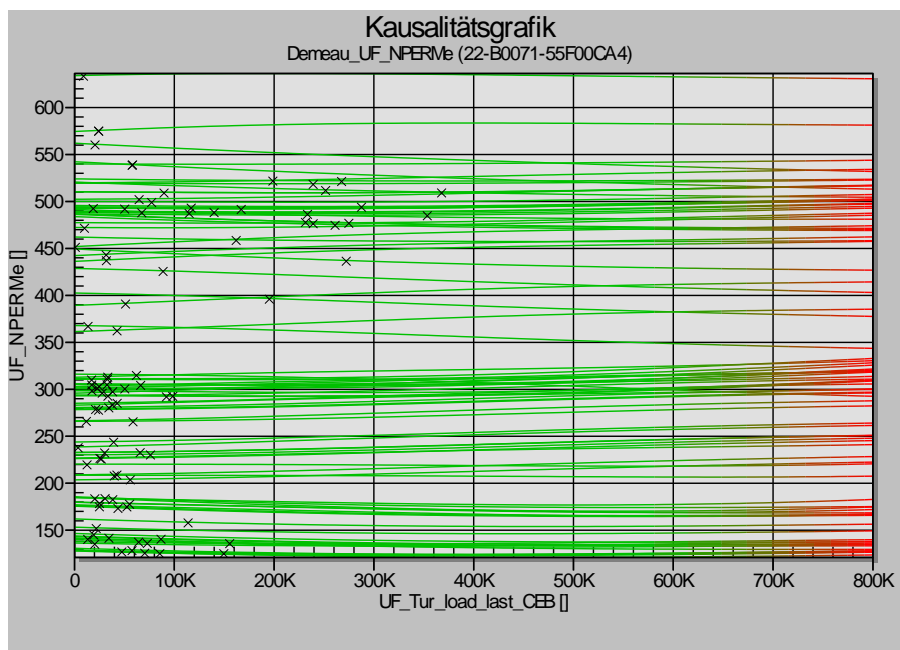


Figure 26: Sensitivity Curves of Turbidity Load since Last CEB, Target Parameter End Permeability

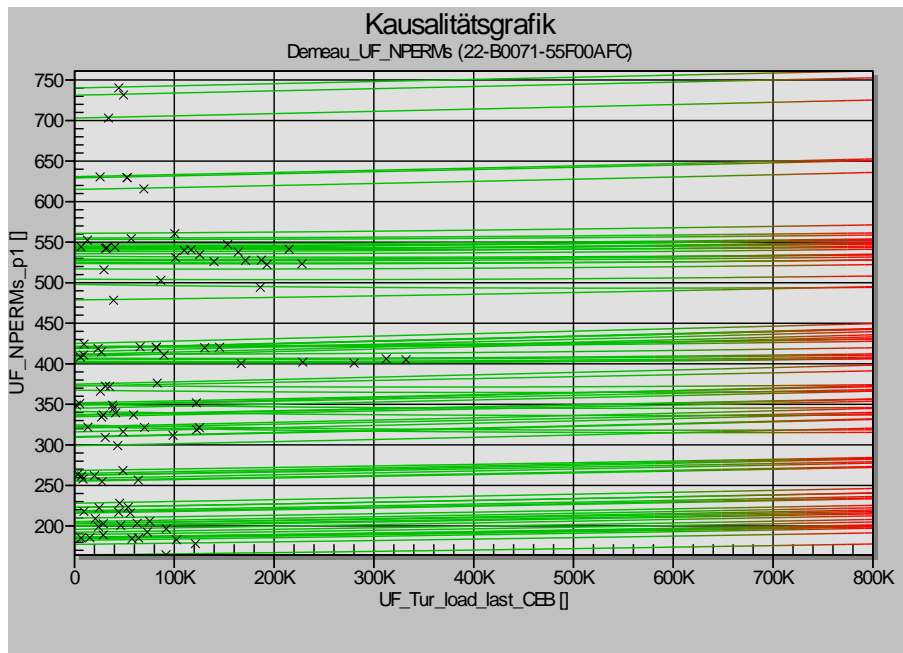


Figure 27: Sensitivity Curves of Turbidity Load since Last CEB, Target Parameter Start Permeability

The curves do not show a significant influence on permeability which indicates that no irreversible fouling occurs. The result is only evidence as the influence may be superimposed by including permeability as input parameter.

2.5 Transfer of the results on the large scale plant

Due to technical reasons and a long delay at the beginning of the project it was not possible to collect experience with ANCS in the large scale plant. The technical reasons correspond to the fact that the staff of the plant in Roetgen is not able to supply us with the needed signals, because the existing PLCs (programmable logical controllers) are nearly completely exhausted relating to memory resources. The procurement and programming of additional PLCs certainly lay outside the scope of our temporal and financial capabilities. Therefore offline optimization of a period of six months from May to November 2014 was considered. To perform this, the transferability of the models of the pilot plant on the large scale plant data has to be tested as the large scale plant is run with constant settings. To enable validation data from large scale plant had to be processed comparable to the pilot plant data. For operating factors data were logged every minute but for water quality data only one hour mean values were available. As the influent was the same as for the pilot plant, pilot plant raw water quality data were therefore merged with the large scale operational data.

As the backwash procedure of 25 s is shorter than the logging interval of one minute for the large scale data only detection of the backwash was possible but no calculation of backwash time and flux could be

conducted. Therefore backwash time and flux were set constant corresponding to the operations diary of WAG. The other parameters were determined as for the pilot plant data. Table 2 shows the data ranges of both plants. As can be seen especially backwash conditions differ significantly and also filtration time shows some deviation at maximum range.

Table 2: Data Ranges of Pilot and Large Scale Plant

Parameter	Pilot Plant		Large Scale Plant	
	Min	Max	Min	Max
Filt_t	900 s	2400 s	1500 s	3480 s
Filt_Q	40 l/m ² /h	110 l/m ² /h	35 l/m ² /h	85 l/m ² /h
BW_t	60 s	75 s	25 s	25 s
BW_Q	100 l/m ² /h	230 l/m ² /h	675 l/m ² /h	675 l/m ² /h
T_av	2,5°C	14,5°C	8°C	17°C
Tur_load_last_CEB	0 l*FNU/m ²	500.000 l*FNU/m ²	0 l*FNU/m ²	26.500 l*FNU/m ²
NPERMs	170 l/m ² /h/bar	880 l/m ² /h/bar	200 l/m ² /h/bar	600 l/m ² /h/bar
NPERMe	100 l/m ² /h/bar	740 l/m ² /h/bar	100 l/m ² /h/bar	500 l/m ² /h/bar

Validation results are shown in the following figures. As for the validation of the pilot plant models the green curves show the measured values and the blue curves represent the calculated model predictions. The percentages refer to the respective ranges of values of the target parameters.

2.5.1 Model of Filtration Subcycle (Target Parameter UF_NPERMe)

The model for the filtration subcycle of the pilot plant is able to predict the progression of data but has considerable deviations especially in the period from May to July (cf. Figure 28). This underestimation is mainly attributed to the differing data ranges of filtration time. The tilt can also be seen in Figure 29 for the correlation graph. Despite the deviation due to differing filtration times it can be stated that the transferability of the pilot plant model to the large scale data is possible for the prediction of permeability at the end of a filtration cycle.

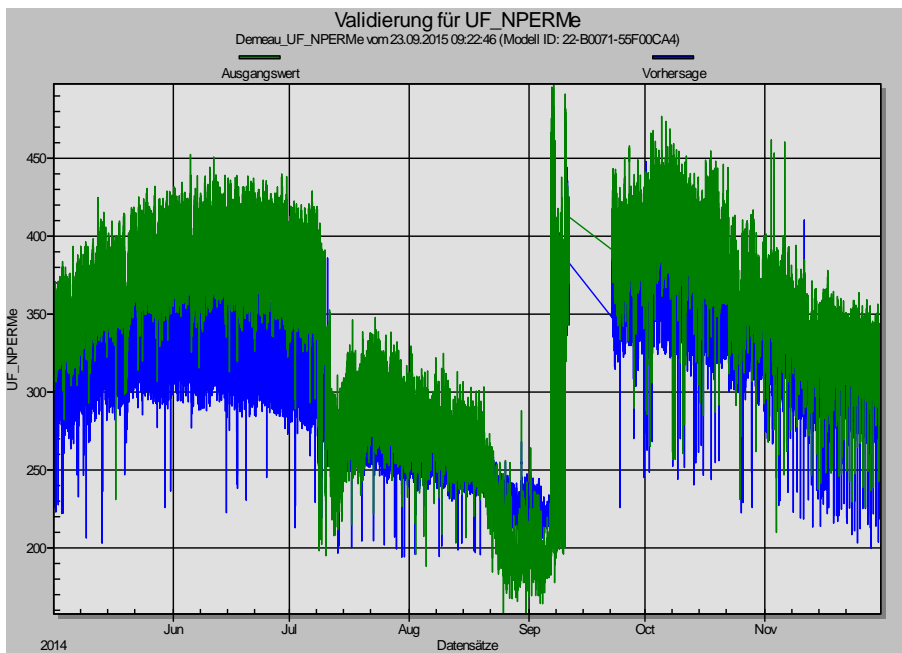


Figure 28: Validation of Filtration Model (Target Parameter: End Permeability) for large scale data

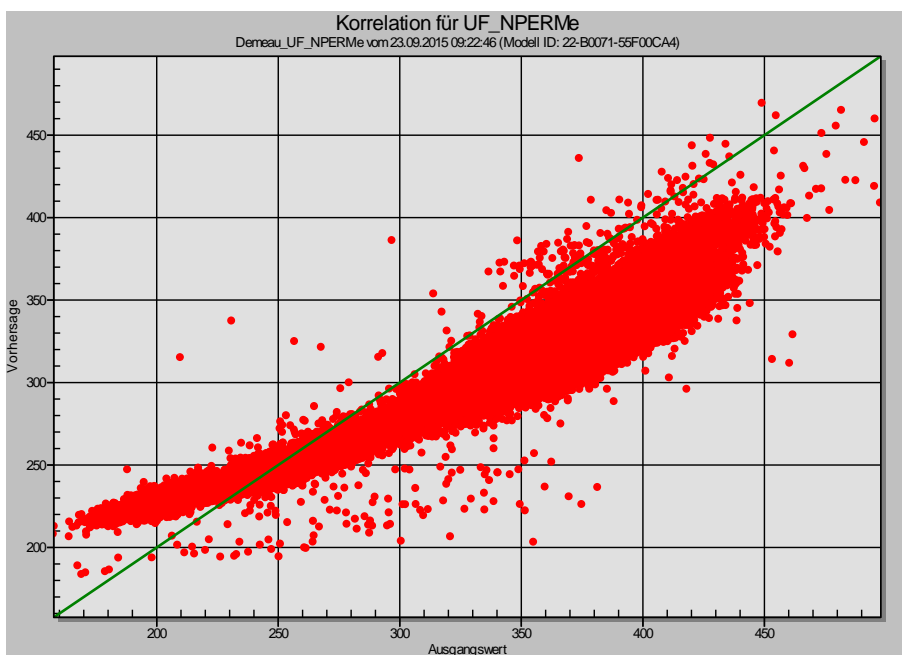


Figure 29: Correlation Graph of Start Permeability for large scale data

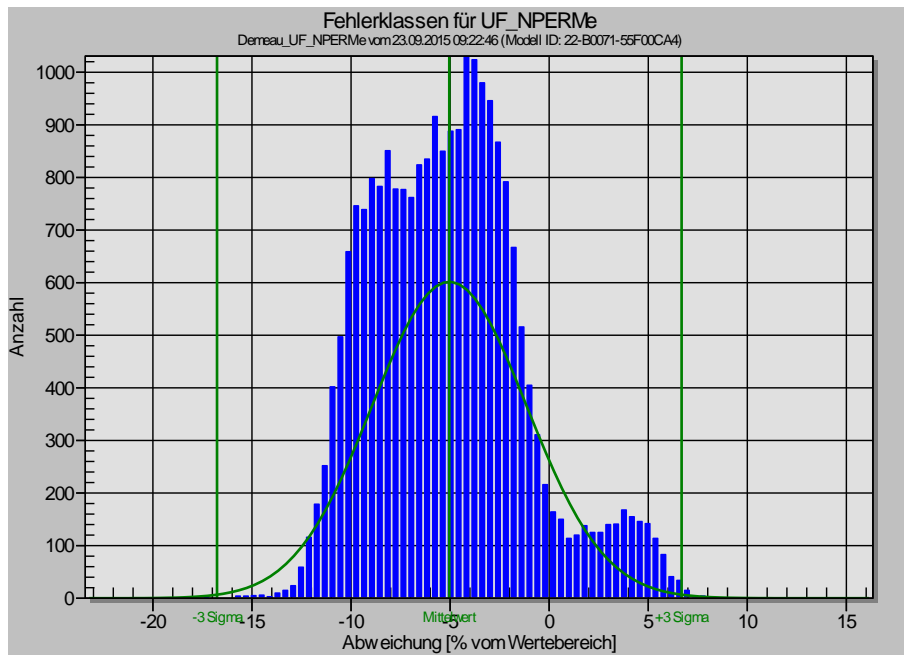


Figure 30: Frequency Distribution of Error Classes of End Permeability for large scale data

2.5.2 Model of Backwash Subcycle (Target Parameter UF_NPERMs)

A comparable image appears for the permeability at filtration start but with much higher deviations due to significant differences in backwash conditions.

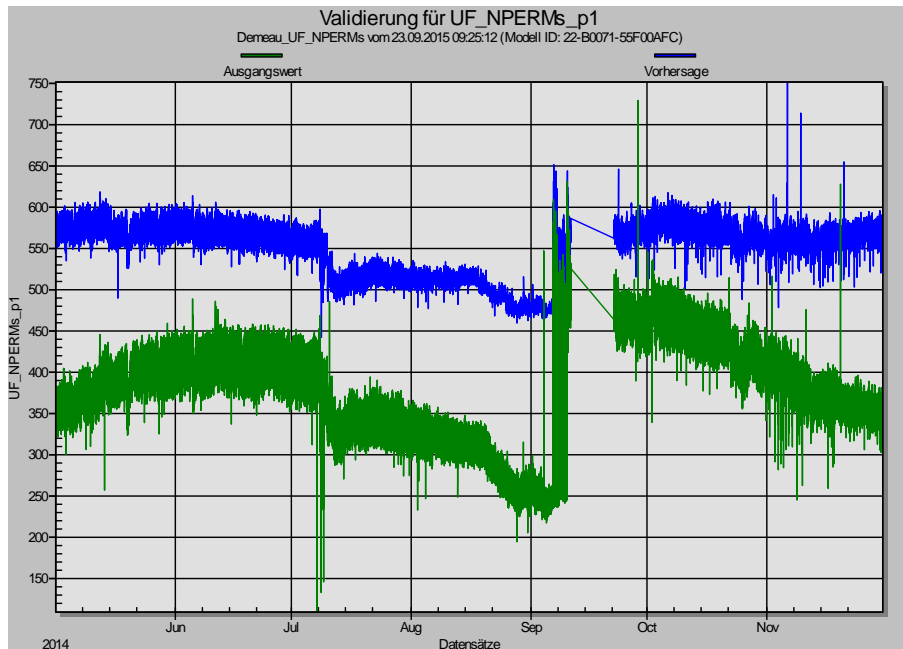


Figure 31: Validation of Backwash Model (Target Parameter: Start Permeability) for large scale data

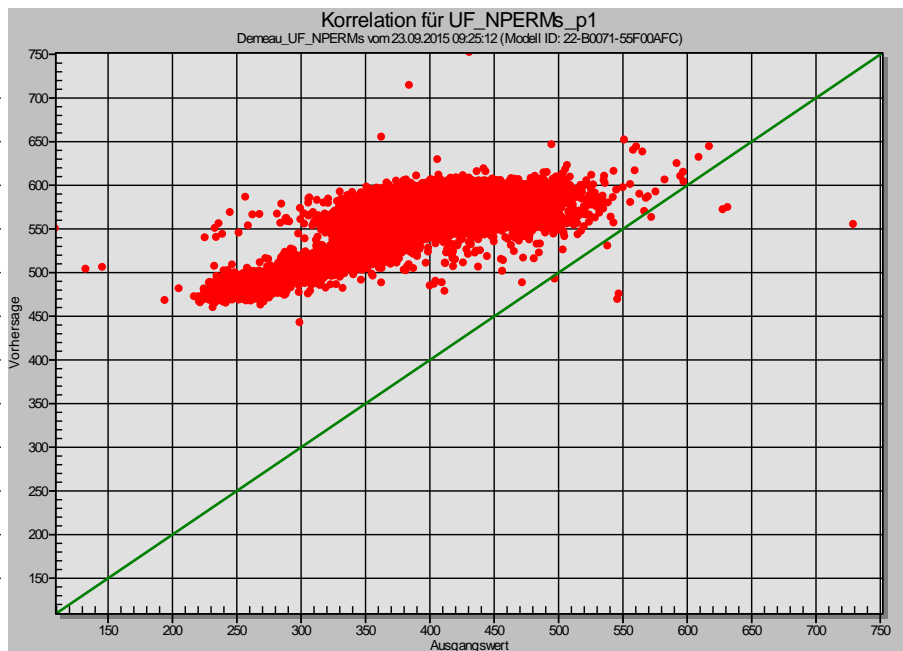


Figure 32: Correlation Graph of Start Permeability for large scale data

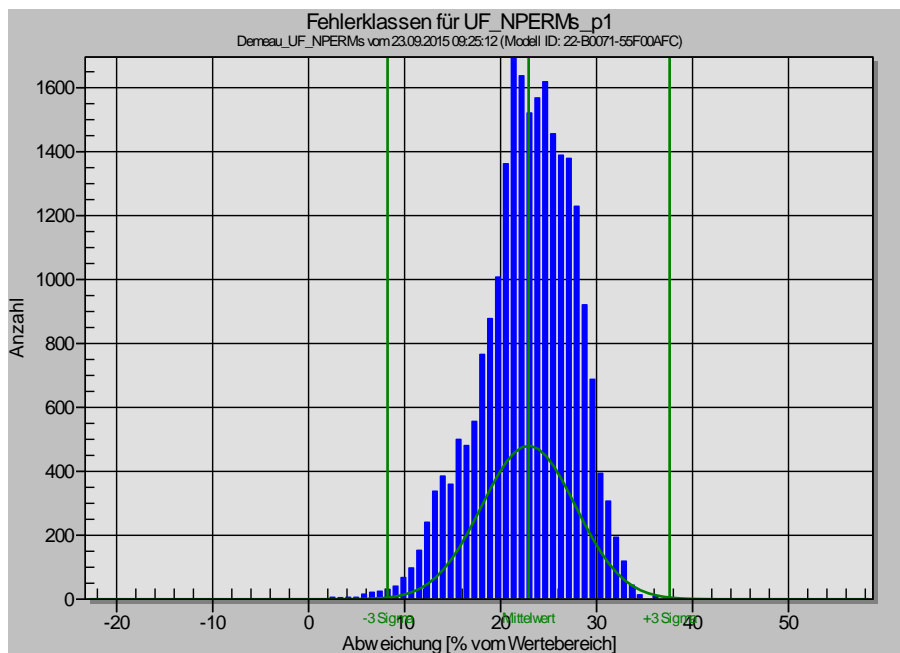


Figure 33: Frequency Distribution of Error Classes of End Permeability for large scale data

2.5.3 Conclusion for the transferability to the large scale plant

Generally the transferability of the pilot plant models on the large scale data is given but due to differing setting ranges deviations appear to be too high for further use of the data for optimization. One possibility to overcome this problem is a retraining of the models with large scale data. A retraining was performed for the permeability at the end of a filtration cycle. The results are shown in the following figures; the statistical parameters are given in Table 3. The deviations are slightly higher than for the pilot plant models. This fact can be attributed to the lower data resolution compared to the pilot plant data.

Table 3: Results of Modelling with Large Scale Data

Name	ID	Date	Mean deviation	Mean absolute deviation	Sigma	RSQ
Demeau_UF_NPERMe	22-B0071-56025A39	23.09.2015	0.15%	2.63%	4.13%	0.97

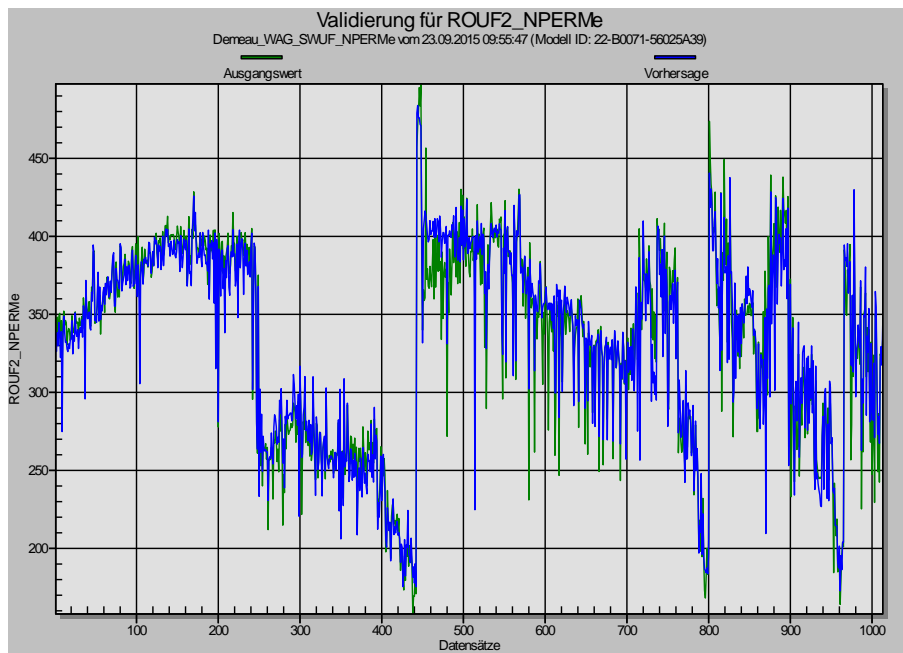


Figure 34: Validation of Filtration Model (Target Parameter: End Permeability) after retraining with large scale data

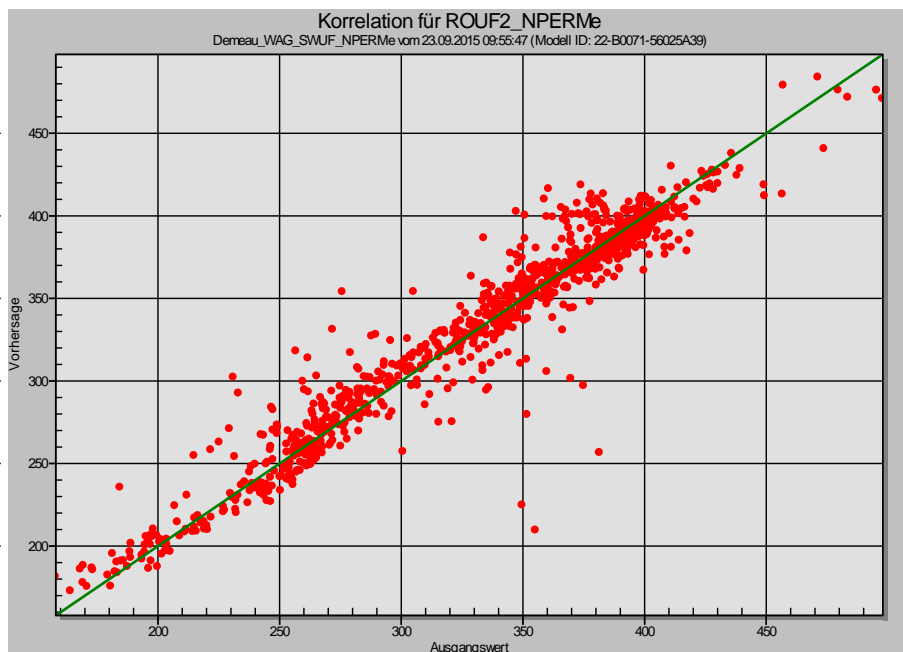


Figure 35: Correlation Graph of Start Permeability for large scale data after retraining with large scale data

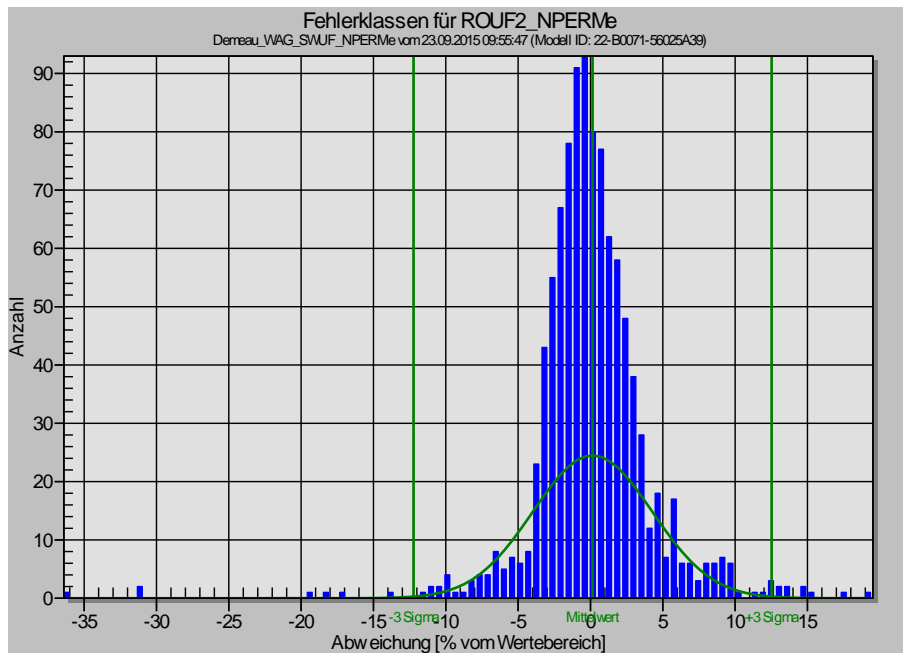


Figure 36: Frequency Distribution of Error Classes of End Permeability for large scale data after retraining with large scale data

The NPERMe-model shows a comparable model quality as for the pilot scale data. The same is to be expected for NPERMs-model but a modelling does not make sense for the objective of optimization as backwash parameters were constant and not exactly determinable so using those parameters as manipulable variable for modelling and optimization did not make sense. Therefore optimization runs were conducted on the basis of pilot plant data.

3 Design of the Optimization System

The results in this chapter show the optimization system for regular backwashes. CEB models were also trained and evaluated within the past report period but the models showed no significant influences of the manipulable variables as the pilot plant in Roetgen was operated with approximately one CEB per day. Due to the high frequency no considerable irreversible fouling could be observed. The normal backwash was able to maintain the permeability on a high level. That means, the frequency of CEB can be reduced significantly in order to save chemicals and increase productivity (the time for a CEB is considerably higher than for a normal backwash – 3.600 sec: 45 sec). Of course the CEB also has important functions concerning disinfection, but from a permeability viewpoint it would be sufficient, to decrease the frequency from daily to weekly or even less. The possible savings are considered to be substantial.

3.1 The Genetic Optimizer

The next illustration shows the genetic optimizer. The optimizer GenOpt Online will access his data out of the APC OPC-Server and perform calculations of forecasts, target function, etc. The results will be transferred back to the APC OPC-Server, from where they will be picked up by APC for further evaluation and display.

The screenshot displays the NeuroModel GenOpt Online 3.1 interface. The main window shows the following data:

Modell
 Projekt: Demeau_UF_Kombi_NPERM - Kombimodell UF100, UF200
 Datei: D:\aquatune\Projekte\EU\01.Demeau\04.Optimierung\Whatif_D23.3\Demeau_UF_Kombi_NPERM.net
 Datum: 09.09.2015 14:19:23

Variablen

Name	Wert	Einheit	Unteres Limit	Oberes Limit	Toleranz	Bias	Verbindung
Eingänge							
UF_Filt_t	2436,91		900	2500	0	0	Optimierer
UF_NPERMs	186,558		150	900	0	0	Handeingabe
UF_Q_av	108,519		40	120	0	0	Optimierer
UF_T_av	5,97705		0	15	0	0	Handeingabe
UF_Tur_load_last_CEB	86772		0	800000	0	0	Handeingabe
UF_Bw_t	56,1775		50	90	0	0	Optimierer
UF_Bw_Q_av	149,405		90	250	0	0	Optimierer
UF_NPERMe_m1	130,843		100	750	0	0	Handeingabe
Ausgänge							
UF_NPERMe	112,22					0	
UF_NPERMs_p1	290,433					0	

Berechnungen

Name	Wert	Berechnung
Productivity	0,969238	(UF_Filt_t*UF_Q_av)/(UF_NPERMs_p1*UF_NPERMe)
TMPs_p1	0,373645	UF_Q_av/(UF_NPERMs_p1*UF_NPERMe)
TMPe	0,967019	UF_Q_av/(UF_NPERMs_p1*UF_NPERMe)
Wel_BW	4,34E-05	((TMPs_p1*UF_Bw_Q_av)/UF_Filt_t)
Wel_Filtration	0,001580	((TMPs_p1*UF_Q_av)/UF_Filt_t)
TMPs	0,58169	UF_Q_av/(UF_NPERMs_p1*UF_NPERMe)
cost_water_BW	0,000419	UF_Bw_Q_av*UF_Bw_t
cost_Wel	2,71E-07	(Wel_BW+Wel_Filtration)*UF_Q_av
Revenue	0,012802	((UF_Q_av*UF_Filt_t)/(UF_NPERMs_p1*UF_NPERMe))

Schranken

Schranke	Quote
UF_NPERMs_p1 > UF_NPERMe	151

Externe Variablen

Name	Wert
Meas_UF_100_Productivity	0,93
rate_Energy	0,167
rate_water	0,18

Optimierer

Fitness: 0,0327994
 Max. Generationen: 1500
 Bereits durchlaufen: 1051
 Quote Schranken: 151
 Quote SecurityNet: 2056

Zielfunktion
 (cost_water_BW+cost_Wel)/(Revenue+0,0000001) -> Minimum

Buttons: Neu, Löschen, Einstellungen, Variablen, Zielfunktion

Status: Optimierung läuft ...

Figure 37: Genetic Optimizer

In the top left of the picture the inputs and outputs of the used model are displayed. Green parameters are disturbance variables coming from the OPC clients or in case of offline WhatIf-optimizations from table inputs. Blue parameters are manipulated by the genetic algorithm in order to fulfil its target function. Below the model there is a window called barriers (Schranken). Here are the boundary conditions implemented which have to be respected by GenOpt. In the above shown the only boundary condition to be observed is that start permeability after backwash has to be higher than end permeability before backwash. This boundary prevents the optimizer to use invalid parameter combinations in areas without sampling points.

The window “Zielfunktion” shows the target function.

3.2 Optimization Strategy

The scheme in Figure 38 illustrates the costs for the ultrafiltration process. The consumed energy that can be influenced by ANCS is based on the product of transmembrane pressure and hydraulic flow rate. Feed side pressure that has to be delivered by the pump is higher than the TMP but is a plant’s constant and is therefore not controllable. Additional costs are generated by backwash water opposed by the gain of filtrated water. In Roetgen filtrated water is lead back to the drinking water treatment plant while the backwash water is thickened and dewatered. As the costs for sludge disposal are not controllable and the clear water phase is disposed to the receiving water only costs for pumping from reservoir have to be considered.

The basic optimization approaches are given by a minimization of energy consumption or a maximization of productivity. Increased productivity will lead to increased energy consumption while less energy consumption decreases productivity. Optimal savings can be reached with balancing energy costs and backwash water costs against increased productivity.

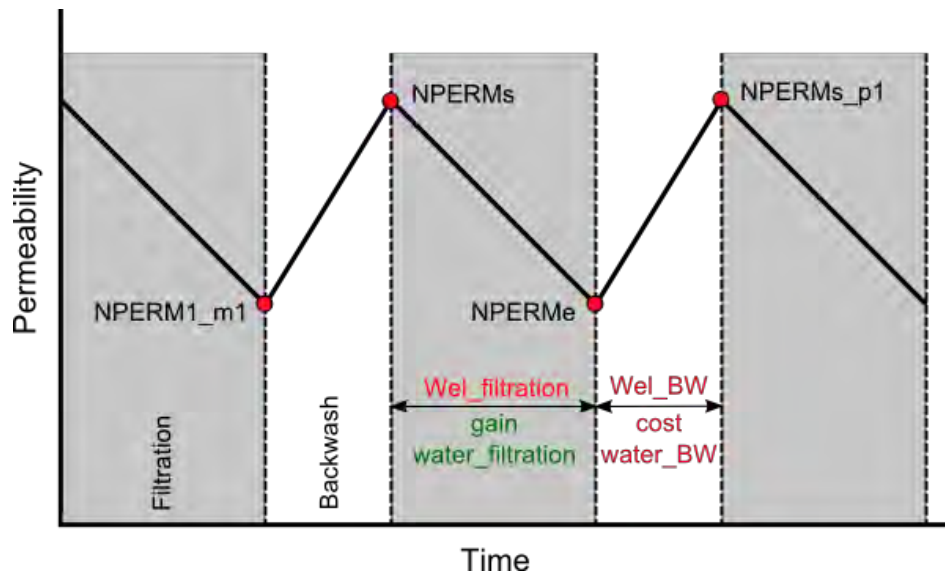


Figure 38: Scheme illustrating costs and gain during a filtration cycle

In detail the target function is calculated by:

$$Target_Function = \frac{Backwash_{cost} + Wel_{cost}}{Revenue} \rightarrow Minimum$$

with:

$$Backwash_{cost} = \frac{BW_Q \left[\frac{l}{h} \right] * BW_t[s] * a \left[\frac{\text{€}}{m^3} \right]}{1000[m^3] * 3600[s]}$$

$$Wel_{cost} = (Wel_{BW}[kWh] + Wel_{Filtration}[kWh]) * b[\text{€/kWh}]$$

$$b = Cost\ per\ kWh \left[\frac{\text{€}}{kWh} \right]$$

$$Wel_{BW} = ((TMPs_p1[mbar] * UF_BW_Q_av \left[\frac{l}{h} \right] * UF_BW_t[s]) + (0,5 * (TMPE + TMPs_p1)[mbar] * UF_BW_t[s] * UF_BW_Q_av \left[\frac{l}{h} \right])) / 3600 / 1000 / 36$$

$$Wel_{Filtration} = ((TMPs[mbar] * UF_Q_av[\frac{l}{h}] * UF_Filt_t[s]) + (0,5 * (TMPe + TMPs)[mbar] * UF_Filt_t[s] * UF_Q_av[\frac{l}{h}]))/3600/1000/36$$

$$Revenue = \frac{Filt_Q [\frac{l}{h}] * Filt_t [s] * a [\frac{\text{€}}{m^3}]}{1000[m^3] * 3600[s]} - Backwash_{cost}$$

$$a = Revenue \text{ per } m^3 [\frac{\text{€}}{m^3}]$$

Since the efficiency factor of the used pump was unknown it was not used. The calculated energy costs will therefore be underestimated and thus the real energy costs and savings will be slightly higher.

This configuration induces the optimizer to find the best compromise between reduced energy consumption and reduced productivity by decreasing the sum of the costs and increasing the revenue (productivity). The trade-off can be controlled by the configured cost factors “b” for energy and “a” for loss of productivity.¹

These factors can be adjusted during runtime and though in the given optimization they represent real costs they can also be used as parameters detached from their real values to shift priorities. If for example there is a high need for produced water, the cost factor “a” could be increased, which would result in more emphasis on productivity and less emphasis on energy costs. In times of excess water the reverse adjustment could be done. Depending on site specific requirements other aspects for optimisation as water availability could also be implemented in the target function in a comparable way.

3.3 Optimization results

Following three optimization runs were conducted:

- Minimization of costs for energy and backwash water
- Maximization of productivity
- Balancing energy consumption against revenue

The optimization was configured without any restrictions to productivity ensuring to find the best result relating to the target function. The only restriction forced the optimizer to observe that permeability at

¹The values for “a” and “b”, that were used, were communicated by the operational staff of the Roetgen plant.

filtration start has to be higher than at filtration end for the purpose to prevent the optimizer to find a wrong optimum. Additionally security net (Froese 1997) was used which ensures that the optimizer only considers optimization proposals for predictions of NPERMs_p1 and NPERMe with a secure confidence interval.

The optimization results can be found in Table 4. Productivity is calculated based on the data used for optimization runs. As they only contain regular backwash cycles but no CEBs real productivity is lower than the calculated as CEBs are much longer than regular backwashes.

Costs minimization relates to the costs per filtration and backwash cycle. As this calculation does not contain any information on productivity savings are much lower than for the other two approaches. Both optimizations for maximization of productivity as well as minimization of costs in relation to revenue lead to equal results. The reason for this is the insignificant costs for energy consumption which is given by TMP which is in the order of a few hundred mbar. Therefore also minimization of costs in relation to revenue results in a maximization of productivity.

Savings of about 70 % are very high but presumably not completely achievable. The optimization is a one cycle optimization without respect to following filtration cycles. Long term effects cannot be represented by the ANN up to now as irreversible fouling was negligible in pilot plant’s trials but may occur when optimization proposals are transferred. The inclusion of irreversible fouling in the ANNs would be part of a retraining of the networks. Conservative estimations for savings range about 30 %.

Table 4: Optimization results (Filtrated Water amounts to about 4.3 Mio. m³/a)

	Total Costs [€/m³ Filtrated Water]	Total Costs Large Scale Plant [€/a]	Savings	Productivity
Measured Value	0,0143 €	61.539 €		93 %
Costs Minimization	0,0110 €	47.461 €	23%	94%
Maximization Productivity	0,0044 €	19.085 €	69%	98%
Minimization Costs/Revenue	0,0044 €	19.077 €	69%	98%

Following figures show the optimization results for manipulable variables and start and end permeability. All figures contain data for UF100 as well as for UF200 as they shall show the tendency of optimization approach which is comparable for both plants.

Filtration time can be increased to maximum values in order to maximize productivity (cf. Figure 39). In case of costs minimization filtration time is adjusted differently for each cycle and covers the whole data range of set points during trial period.

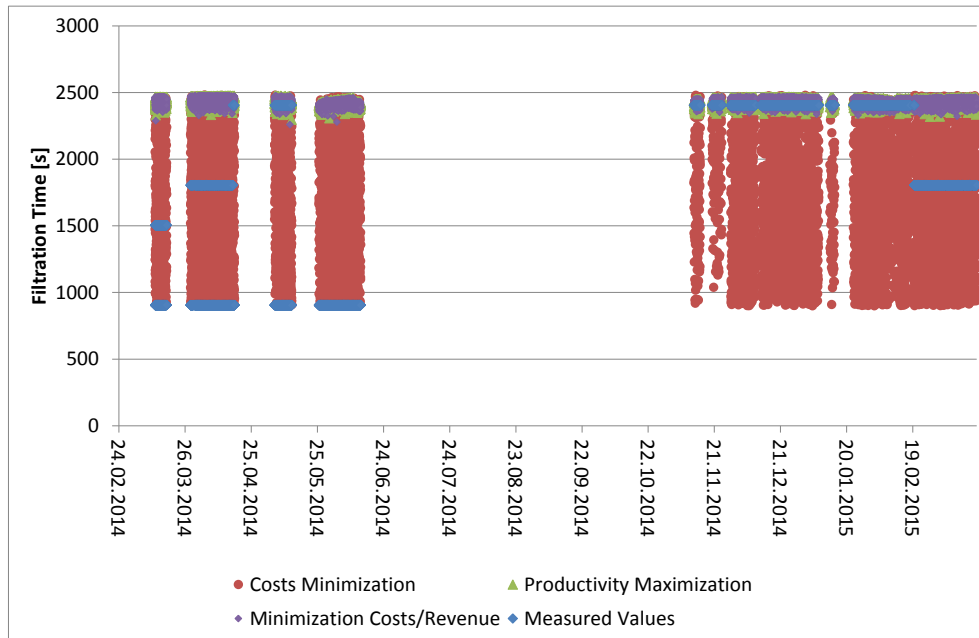


Figure 39: Optimization of filtration time

As for filtration time filtration flow is also adjusted differently each cycle in case of costs minimization while flow is maximized for both of the other optimization approaches. Only at a short period in July before the wide time gap a short period occurs where maximum flow is not proposed, presumably due to restrictions by security net.

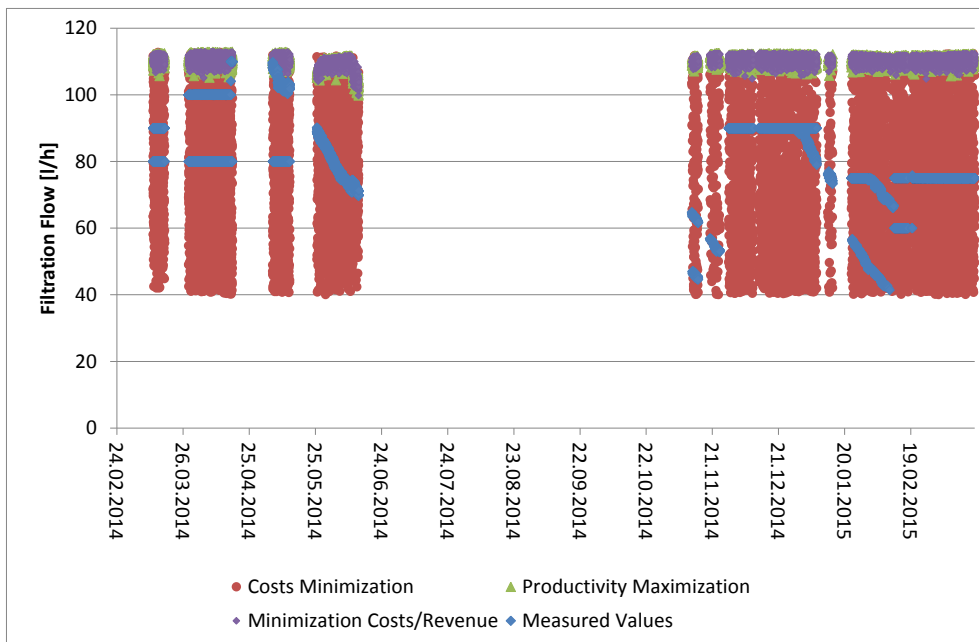


Figure 40: Optimization of filtration flow

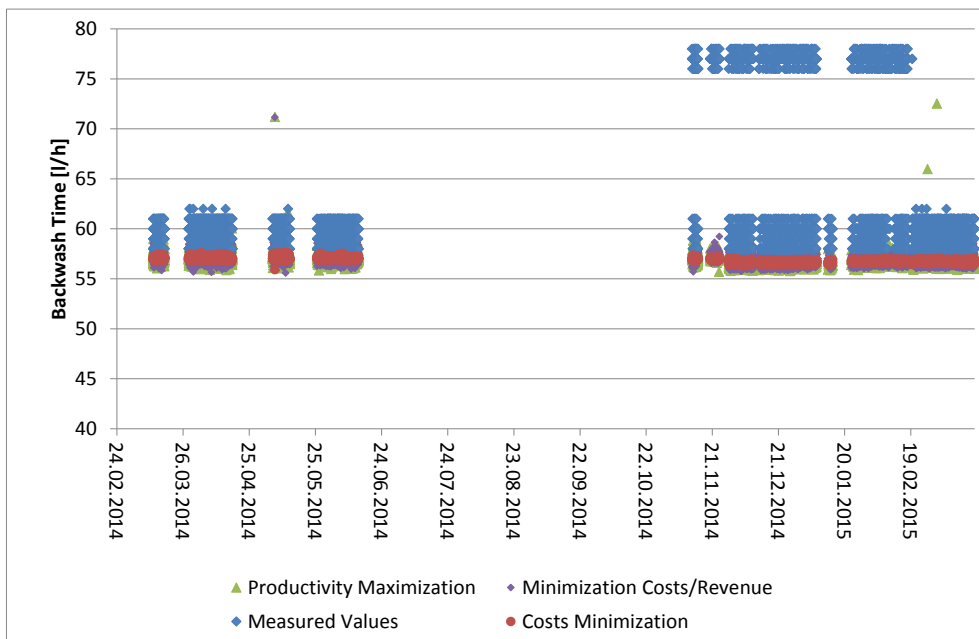


Figure 41: Optimization of backwash time

For all optimization approaches backwash time is proposed to be minimized to the lowest level (cf. Figure 41). This is expectable as backwash water is considered for cost minimization and reduced amount of used water increases productivity.

As only insignificant irreversible fouling occurred during trial period and only one cycle optimization could be executed also backwash flow is proposed to be reduced. From December on an increase of backwash flow can be observed (cf. Figure 42). Proposed values are comparable for all optimization approaches. The parallel curves originate from different proposals for UF100 and UF200 in which the higher curve belongs to UF200. The reason for increased optimization proposals is the application of security net. Without proposals can be expected to be minimal, too but as no patterns were trained for this situation in the ANN the proposal would have been incorrect extrapolation.

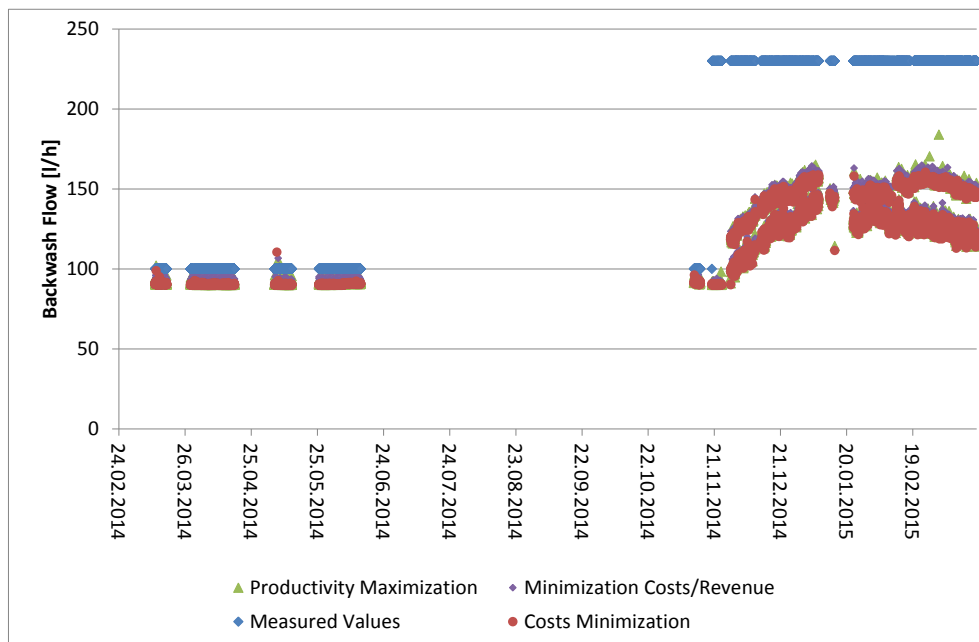


Figure 42: Optimization of backwash flow

Due to increased productivity by increased filtration time and flow permeability at filtration end is expected to be lower after optimization. Variation in permeability for costs minimization is much higher due to changing optimization proposals for filtration time and flow. Also higher permeability than measured can be achieved especially after November 2014.

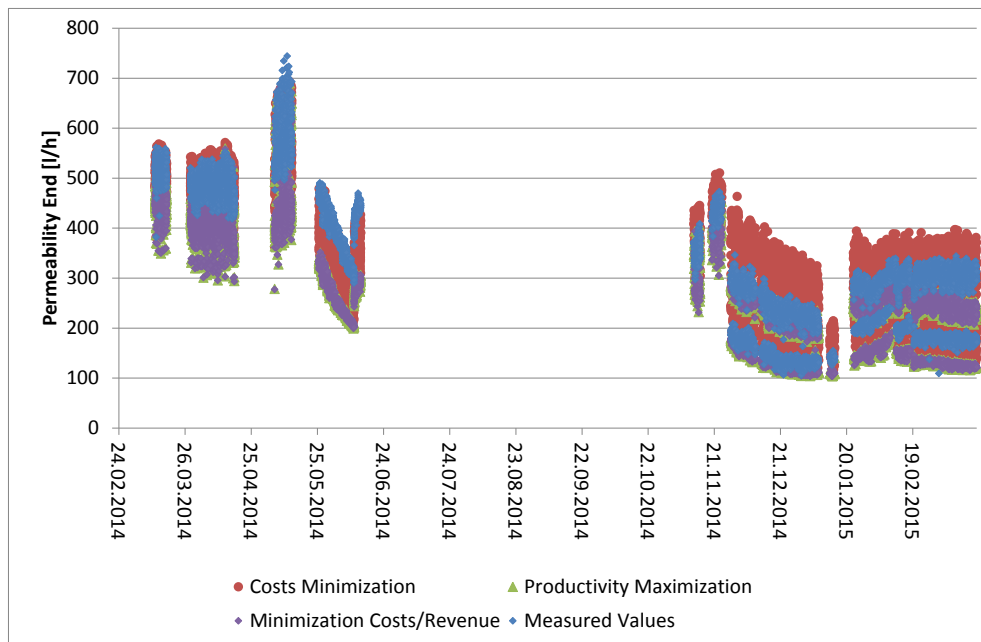


Figure 43: Measured and resulting permeability at filtration end

For permeability at filtration start no significant changes are resulting from set point changes. A little increase can be observed after November 2014 for UF200 which is represented by the lower curve.

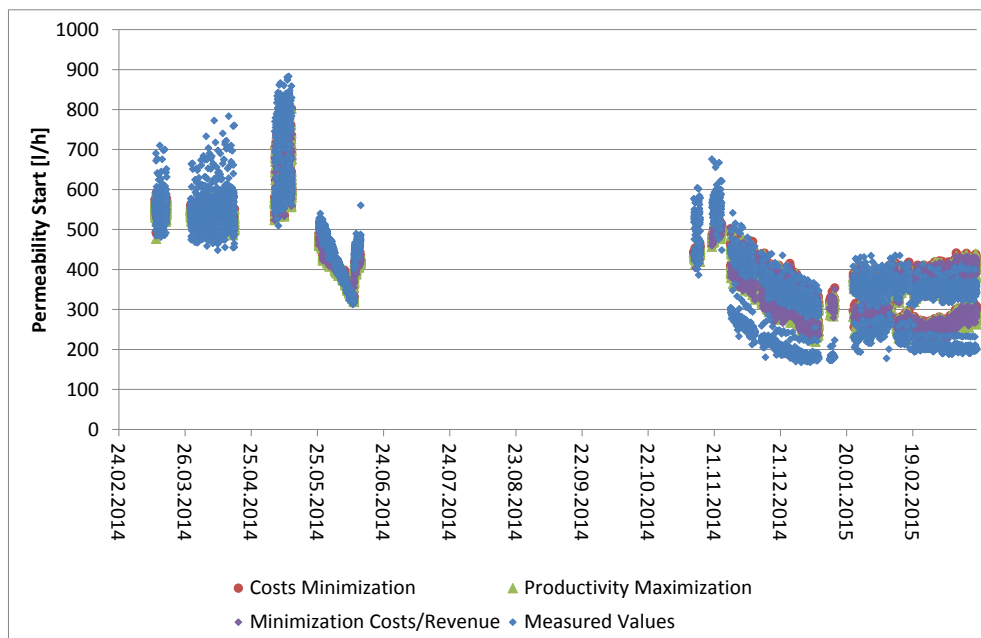


Figure 44: Measured and resulting permeability at filtration start

Productivity is increased to about 98 % and to a little lower level after November 2014 due to higher backwash flow. For Costs minimization big differences are resulting from varying optimization proposals for filtration time and flow. Productivity can be less than measured values.

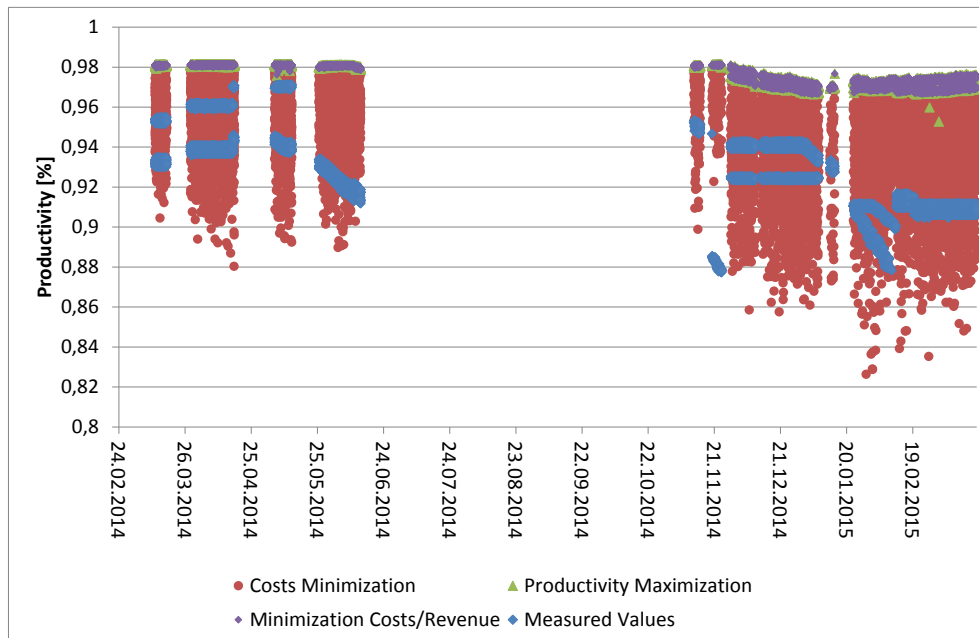


Figure 45: Productivity before and after optimization

Table 5 summarizes the optimization results. Interpreting the tendencies it has to be considered that nearly no irreversible fouling occurred at the pilot plant so that considerable changes for the operational parameters were possible.

Table 5: Summary of the optimization results with respect to the real settings

	filtration time	filtration flux	backwash time	backwash flux	Productivity	Savings
Costs Minimization	individually adapted	individually adapted	decreased	decreased	reduced	low
Maximization Productivity	increased	increased	decreased	decreased	increased	high
Minimization Costs/Revenue	increased	increased	decreased	decreased	increased	high

4 Conclusions

The automatic neural net control system (ANCS) for UF membrane filtration can be implemented with ANN models of high prediction accuracy for the prediction of permeability at filtration start and filtration end depending on water quality parameters and the operational parameters filtration time and flux as well as backwash time and flux. Latter are manipulable variables that can be adjusted by ANCS' optimization system. The results can be transferred to comparable plants. The ANNs have to be trained the same way as shown above with site specific data potentially enhanced by additional input parameters to represent different raw water quality or include other process parameters like e.g. CEB if necessary. Once ANCS is adapted to site specific conditions and implemented in the process, maintenance requirements are quite low as the system can be adjusted to new process conditions by retraining the ANNs with new data. For full utilizability as control system the only requirement is a variation of operational parameters as ANNs are data driven and represent what is included in the training data set with only slight extrapolation.

For the optimization system different approaches like costs minimization, productivity maximization and minimization of costs versus revenue are possible. The optimization results of this study show the benefit of productivity maximization also due to the fact that influenceable pressure for energy minimization, namely TMP, is quite low and therefore costs are insignificant compared to costs for backwash water.

References

- aquatune GmbH, (2005): Standard-Ablaufschema Neuro-Projekte – Predictoren / Virtuelle Sensoren / Prozessmodelle, Engineering Norm 0010596, Version 4, Revision 2
- Froese, T. (1997): Verfahren zur Erkennung von fehlerhaften Vorhersagen in einer neuromodell-gestützten oder neuronalen Prozessregelung. European Patent EP 0 762 245 A1
- Mälzer, H.-J., S., S., Gebhardt, J., Nahrstedt, A., Panglisch, S., Gimbel, R., Zach, W. (2008): Artificial Neural Networks for online control of coagulation in drinking water treatment. World Filtration Congress 10, Leipzig
- Panglisch, S., Strugholtz, S., Rohn, A., Mälzer, H.-J., Nahrstedt, A., Dördelmann, O., Becker, A. (2008): Neuronale Netze in der Membranfiltration. Bundesministerium für Bildung und Forschung (BMBF) Forschungsvorhaben 02 WT 0661 (Hrsg.)
- Purifast (2012): Advanced Purification Of Industrial And Mixed Wastewater By Combined Membrane Filtration And Sonochemical Technologies, EU Life Project LIFE07 ENV/IT/000439
- Strugholtz, S., Panglisch, S., Gebhardt, J., Gimbel, R. (2006): Modeling and optimization of ceramic membrane microfiltration using neural networks and genetic algorithms. Water Practice & Technology 1(4)
- Strugholtz, S., Panglisch, S., Gebhardt, J., Gimbel, R. (2008): Neural networks and genetic algorithms in membrane technology modelling. Journal of Water Supply: Research and Technology - AQUA 57(1), 23-34